Programmable Atom Equivalents: Atomic Crystallization as a Framework for Synthesizing Nanoparticle Superlattices

Programmable Atom Equivalents: Atomic Crystallization as a Framework for Synthesizing Nanoparticle Superlattices

Paul A. Gabrys, Leonardo Z. Zornberg, Robert J. Macfarlane*

P. A. Gabrys, L. Z. Zornberg, Assistant Prof. R. J. Macfarlane
Department of Materials Science and Engineering, Massachusetts Institute of Technology (MIT), 77 Massachusetts Avenue, Cambridge, Massachusetts 02139, United States
E-mail: rmacfarl@mit.edu

Decades of research efforts into atomic crystallization phenomenon have led to comprehensive understanding of the pathways through which atoms form different crystal structures. With the onset of nanotechnology, methods that use colloidal nanoparticles (NPs) as nanoscale "artificial atoms" to generate hierarchically ordered materials are being developed as an alternative strategy for materials synthesis. However, the assembly mechanisms of NP-based crystals are not always as well-understood as their atomic counterparts. The creation of a tunable nanoscale synthon whose assembly can be explained using the context of extensively examined atomic crystallization would therefore provide significant advancement in nanomaterials synthesis. DNA-grafted NPs have emerged as a strong candidate for such a "programmable atom equivalent" (PAE), because the predictable nature of DNA base-pairing allows for complex yet easily controlled assembly. This review highlights the characteristics of these PAEs that enable controlled assembly behaviors analogous to atomic phenomena, which allows for rational material design well beyond what can be achieved with other crystallization techniques.

1. Introduction

The field of materials synthesis has historically been dominated by the development of new methods to control material structure that use atoms as building blocks and crystallization as a driving force for the formation of higher levels of ordering.[1,2] The diversity of the resulting materials is derived from a periodic table that is filled with a multitude of different atoms with

different chemical identities, sizes, and bonding behaviors.[3–5] The kinetic and thermodynamic organization of atoms into these complex materials is well-studied, and therefore known to follow rational and (in simple cases) predictable pathways towards crystalline architectures.[6–9] As materials science and chemistry have expanded in recent decades to include the development of nanotechnology as a driving principle for materials discovery, new building blocks based on nanoparticles (NPs) have emerged as a means to further control the complexity of material structures across a wide range of size regimes.[10–13] However, the assembly of these nanomaterial synthons can be governed by many different chemical and physical forces,[14–20] and this increased level of complexity in NP assemblies is not nearly as well-understood or examined as the atomic crystals that came before them. Therefore, atomic crystallization behavior would be an ideal template upon which to model a framework to understand and program NP-based superlattices and bulk materials. The development of a set of nanoscale "atoms" that can be rationally directed into ordered assemblies with well-defined, hierarchical structures on length scales orders of magnitude larger than the individual building blocks would constitute a major step forward in the field of materials science. While multiple means of controlling NP assembly have been developed, correlating NP assembly behaviors to known atomic crystallization phenomena would require nanoscale "atoms" with several key design features that would allow for rational control over their formation into larger structures. NP building blocks that have well-defined compositions, sizes, shapes, and predictable binding interactions that dictate their local coordination environment would allow for complete control over material structure at the nanometer and larger scales. Moreover, if the assembly process truly mimicked atomic crystallization, it would allow for rational exploration of crystallization behaviors that are often difficult to study, like defect structures, surface faceting, or kinetic mechanisms of crystal growth.

While multiple types of ligands have been grafted to NP surfaces to control their assembly,[16,18–21] this review will posit that the most programmable means of dictating NP

superlattice formation is the development of DNA-grafted NPs as "programmable atom equivalents" (PAEs). Specifically, we will outline the history of PAE crystallization, focusing on how the use of nucleobase pairing between surface-grafted oligonucleotides has developed from a simple means of aggregating NPs to a now completely controllable process for synthesizing complex hierarchical structures. These PAE building blocks follow crystallization phenomena that are remarkably similar to those exhibited by atoms, but the predicable and synthetically manipulatable DNA base-pairing interactions allow their assembly to be controlled in a means that is entirely impossible for atomic systems **(Figure 1)**. As a result, the moniker of "programmable atom equivalent" is incredibly apt for this nanomaterial building block; we will demonstrate both how they have developed into a powerful materials synthon and highlight key areas of investigation that promise exciting discoveries in the fields of both chemistry and materials science.

1.1. "Atom-Like" Behavior in Colloidal Crystals

The concept of utilizing NPs to mimic atoms is not unprecedented, as the term "artificial atom" has been used to describe colloidal assembly systems for many years.[22] Early discoveries found that colloidal particles would undergo "solid-liquid-gas" phase transitions based on changes in NP concentration and relative interaction strengths between NPs, where the different phases were defined by the relative mobility and ordering parameters of the colloids.[23–25] More recently, "artificial atoms" with directional binding akin to molecular valency have been explored via the creation of "patchy particles" that express multiple types of ligands at different points across their surfaces or possess particle cores with specific polyhedral or anisotropic shapes.[26–30] However, all of these classic examples of "atom-like" behavior in colloids are limited to analogies in narrow circumstances. In particular, they do not always crystallize into materials with long range order or often provide just a singular example of crystallization that is not generally applicable to the formation of multiple different structures. The predominant methods to assemble these particle-based periodic structures are *via*

evaporation or sedimentation of ~100-1000 nm colloids.[14,31] During this process, spherical particles close pack together due to solvent exclusion and maximization of entropy, generally yielding face-centered cubic (fcc) structures, as this structure represents the densest arrangement of hard spheres.[13,32]

Driven by the desire to harness the powerful driving force of crystallization in creating different periodic structures beyond just fcc lattices, significant research has been devoted to creating ordered superstructures (superlattices) of colloidal NPs with several different coordination environments. The technique of slow-drying a solution of colloids onto a substrate has proven particularly effective in producing several different crystal forms, at least in 2D NP thin films. To achieve this, uniform NPs (dispersity typically less than 5%) must be synthesized such that they will close-pack together into space filling arrangements.[33] Using the slow-drying method, both molecule- and macromolecule-grafted NPs have been shown to yield a large breadth of different crystal structures from dried mixtures of one,[17] two,[16,34] or even three NP components.[35] Complex arrangements like quasi-crystalline superlattices have been achieved with this method as well.[36] These crystalline symmetries have even been shown to be achieved with multiple NP compositions,[34,37] broadening the programmability of these NPs as "artificial atoms." Nevertheless, while NPs of various compositions, sizes, and shapes can be used in various mixtures,[33] the final coordination environment cannot be directly programmed into the building block using this methodology. In other words, the structures that are achieved are inherently linked to the identities of the NPs being assembled and cannot be purposefully manipulated to yield a different crystalline arrangement without changing the NP size, shape, etc. The achieved crystalline phases have been retroactively explained to a remarkable level of certainty, though typically based on arguments of space-filling and maximization of ligand entropy.[38] Other systems using charged colloidal NPs and ionic attraction have been developed to harness explicit enthalpic attractive forces to govern interparticle interactions,[15,18,39] but these motifs require that only very short interparticle

distances be used, meaning that the achievable arrangements are similarly restricted by the identity of the underlying NP. While effective at mimicking specific atomic behaviors, these "artificial atom" systems do not have the level of programmability required from a building block that could truly take advantage of atomic crystallization behavior and harness it to control structure.

1.2. Moving Beyond "Artificial Atoms"

For the purposes of this review, we would set the definition that the difference between a nanoscale "artificial atom" and a truly "programmable atom equivalent" is that a *programmable* building block must be modular, meaning that the moiety controlling the interparticle interactions must be entirely separate from the underlying NP identity (size, shape, composition). In other words, the synthesized building block must yield a direct output (i.e. crystalline unit cell) from a specific and intentionally designed input (i.e. programmed interparticle interaction). "Artificial atoms" (Section 1.1) have proven very successful in *correlating* specific aspects of the building block design to resulting crystalline architectures, enabling significant insight into colloidal crystallization behaviors and the synthesis of many unique materials. However, none of these motifs allow for the independent *manipulation* of NP coordination environments without adjusting variables such as NP size and shape. The above examples do demonstrate that self-assembly of colloidal NPs can remove some aspects of the NP's identity, particularly composition, from their coordination characteristics, but a higher degree of programmability is required to truly predict, control, and tune crystal formation. Ultimately, a building block that could rationally control particle assembly in such a manner would not be considered simply an "artificial atom" but a fully programmable atom equivalent.

The use of DNA as a directing force for NP assembly was originally conceived and demonstrated over twenty years ago.[20,40] As a ligand, DNA can be synthesized with molecular purity and with unparalleled precision in monomer sequence. Mirkin *et al.* originally demonstrated that a DNA-grafted NP could be used to rationally design nanomaterials and

precisely program crystalline NP superlattices,[20] as the DNA corona would dictate specified binding interactions to determine which NPs would form bonds with one another.[41] In the subsequent decades, this modular, tunable building block design has indeed become a powerful synthon in nanomaterials synthesis and has been used to assemble multiple different crystalline architectures, earning it the title Programmable Atom Equivalent (PAE). To fully understand the PAE's potential as a materials building block, we will first discuss their design features that allow PAEs to crystallize in a predictable manner that bears many analogies to atomic crystallization.

2. The Characteristics of a "Programmable Atom Equivalent" (PAE)

2.1. Discrete Nanoscale Arrangement of Oriented DNA Provides Multivalency

In the broadest sense, a PAE is defined as a particle of any shape and composition densely functionalized with a monolayer of synthetic oligonucleotides of designated base-pair sequence **(Figure 2A)**. The first examples of such particles demonstrated that the addition of "linkers" could selectively program NP aggregation into clusters[40] or aggregates with no long range order.[20] The original design used two non-complementary single-stranded DNA (ssDNA) anchors on gold NPs (AuNPs) such that they would only undergo selective aggregation upon the addition of "linker" strands designed to duplex to the strands anchored on the NPs (Figure 2B).[20] AuNPs were used in these initial studies because gold-thiol chemistry can be used to easily and readily attach a large number of oligonucleotides to each NP. Additionally, AuNPs possess a surface plasmon resonance that is sensitive to its local environment, meaning that aggregation is easily monitored by UV-Vis Spectroscopy.[42] The earliest work done on these materials was to maximize their colloidal stability by increasing the DNA loading and strength of the DNA-Au attachment chemistry. Using fluorophore-labeled linkers, the surface coverage of DNA on the AuNP surface could be quantified,[43,44] and modifications to the oligonucleotide sequence or the chemical structure of the oligos (e.g. incorporation of polyethylene oxide spacer groups[45]) were investigated as a means of

controlling the grafting density at the particle surface.[46] Importantly, DNA loading was found to be dependent on steric hindrance between grafting strands,[47] and a key innovation to increase loading density was therefore to slowly shield the negatively charged DNA backbone with the addition of sodium chloride during the functionalization process (salt aging).[45] This ultimately enabled a maximum grafting density of 56 pmol/cm^2, which has been demonstrated to be critical in the use of PAEs for materials synthesis by enhancing the degree of multivalency between bonded PAEs.

Although an early goal for PAEs was to be able to use them to programmably build highly ordered nanostructures, the complexity of this new building block made this goal challenging, requiring a significant amount of investigation into the properties and behavior of PAEs as a function of their particle and oligonucleotide designs. As a result, early studies involving PAEs exploited their ability to selectively bind to DNA for sensing[48–51] and biomedical applications.[52–54] It was discovered early on that the arrangement of multiple oligonucleotides in a brush architecture around a nanoscale scaffold imparted higher binding constants,[55] greater discrimination against nucleotide mismatch,[56,57] and even enhanced cell uptake[58] and biocompatibility.[59,60] Due to these new properties that arise as a function of nanoscale geometry and multivalent binding behavior, the DNA-grafted particles were coined "Spherical Nucleic Acids"[61] to highlight the unique and important effects imparted by arranging a dense monolayer of oligonucleotides around a nanoscale core.

A key feature of all PAEs is that the DNA duplex structures can be disrupted at elevated temperatures, and the particles can therefore be reversibly assembled and disassembled by thermal cycling.[20] Initially, it was observed that overall PAE aggregate sizes grew over time even under static temperatures; this was attributed to an "Ostwald ripening-like" process.[62] Similarly, an investigation of melting transition (T_m) sharpness revealed a dependence of T_m on aggregate size.[63] From these data, it was hypothesized that PAEs on the surface of aggregates must be in flux due to having fewer binding interactions than those in the bulk. This concept of

PAE cooperativity was further corroborated by data revealing that an increased density of "sticky ends" linking the particles to one another (through higher surface loading or geometric factors like NP curvature) resulted in an increased and sharpened T_m[55] and could be capitalized upon to selectively aggregate PAEs of different sizes.[64] The collective nature of PAE binding, where not one but many DNA hybridization interactions exist between two PAEs, allows these building blocks to rearrange and densify when the temperature approaches T_m as observed in both Monte Carlo simulations[65] and experiment,[66] ultimately proving incredibly important in enabling the crystallization of PAEs.

2.2. Cooperativity of DNA "Sticky Ends" Enables Crystallization

The first decade of research into PAE assembly focused primarily on structures with well-defined interparticle interactions but was unable to generate materials with anything more than short range order defined by a constant interparticle distance.[67] In the late 2000s, a common intellectual breakthrough occurred independently in several research groups that enabled the formation of NP superlattices with long-range order.[68–70] The key discovery was that the ability to thermally anneal PAE aggregates into crystalline materials was inhibited by the strength of the individual DNA hybridizations holding them together. When the strength of each thermally-reversible binding interaction is reduced (e.g. shortening the ssDNA "sticky end" at the end of each grafted oligonucleotide from 12 to as little as 4 bases[69]), the rate of sticky end duplex dissociation increases by several orders of magnitude. However, because of the dense monolayer of oligonucleotides on the surface of the particles, the high local concentration of sticky ends results in equally rapid reassociation.[71] As a result, the individual connections between PAEs using these short sticky ends are in a constant state of flux, enabling particles to more rapidly reorganize within an aggregate without fully dissociating from one another. This increased mobility enables the PAEs to reach the enthalpically-driven thermodynamic state that maximizes the overall number of DNA connections (i.e. maximizes the number of complementary nearest neighbor particles) which is typically a periodic, close-packed

crystalline arrangement.[69] The first PAE crystals comprised either a unary system (using PAEs with self-complementary sticky ends) or a binary system (using two sets of equal size PAEs with different but complementary sticky ends) and formed either fcc or body-centered cubic (bcc) crystals, respectively (Figure 2C).[69,70] The fcc lattices were hypothesized to be stable due to the fact that each particle possesses the maximum number of nearest neighbors (and thus the maximum number of DNA connections to adjacent particles). While PAEs in a bcc lattice do not maximize the total number of nearest neighbors, each particle in this binary system does possess the maximum number of complementary nearest neighbors to which they can actually form a DNA bond. While several different DNA design motifs have been shown to successfully crystallize PAEs[68–70,72] (some with slightly different design rules governing their behavior[73]), all rely on the common intellectual principal of maximizing multivalent DNA interactions.

Following this initial breakthrough, a flood of new research began in understanding the basic principles that governed the assembly of crystalline PAE structures, and it was quickly discovered that many of the assembly behaviors closely matched atomic crystallization phenomena that had already been explored. Ultimately, a set of design rules was laid out in 2011 that explained PAE crystallization behavior in a manner similar to Pauling's rules for ionic solids,[6] and a simple "complementary contact model" (CCM) was established to semi-quantitatively explain the stability of different PAE lattice phases.[74] However, unlike Pauling's rules, the CCM developed for PAEs used simple geometric rules to predict the arrangement of particles that maximized favorable enthalpic interactions between DNA strands on complementary particles. As a result, the CCM can actually be used to predict and even program the crystalline lattice favored by a given set of PAEs, yielding a broad phase space of different, experimentally-achievable crystallographic symmetries beyond fcc and bcc.[74] While subsequent investigations have shown that the conformational entropy of the DNA ligands and more complicated aspects of DNA hybridization are required to fully explain all aspects of PAE superlattice formation, their assembly behavior remains highly predictable and controlled,

resulting in an attractive crystallization technique for chemists and materials scientists. The numerous similarities to atomic crystallization and ability to precisely dictate NP superlattice structure ultimately led to the development of the term "programmable atom equivalent" (PAE) to describe these building blocks.[75]

3. Versatility in the PAE Construct[76]

3.1. Modularity of the Nanoparticle Core

One of the major advantages provided by programming NP assembly with DNA is the ability to completely separate the chemical composition of the NP core from the lattice structure that is generated, enabling significant chemical diversity to the materials synthesis process. To date, PAEs have been experimentally synthesized, functionalized, and crystallized with cores of various metals, oxides, polymers, and even biological nano-structures (**Figure 3**). Gold,[20,70,77,78] silver,[79] and silver/gold core-shell[80] NPs are most commonly used, both because their plasmon resonances allow for simple monitoring of assembly, and thiol chemistry enables simple functionalization of particles with a dense DNA monolayer. NPs with luminescent properties (cadmium selenide,[78,81–83] cadmium telluride,[78] and zinc sulfide[77,78] quantum dots), magnetic properties (iron oxide[77,78,84]), and catalytic properties (palladium[78] and platinum[77]) have all also been demonstrated. The breadth of available PAE core sizes has increased with the DNA functionalization of other oxide cores (silica[85,86] and titania[86]) and polymer spheres (poly(styrene) (PS),[68,86–89] poly(methyl methacrylate) (PMMA),[86] and 3-(trimethoxysilyl)propyl methacrylate (TPM)[86]). Even metal-organic-frameworks (MOFs)[90] have been shown as a suitable PAE core material. Intriguingly, "hollow" NPs that lack a solid core have been synthesized using a cross-linking strategy that creates a thin polymer shell around a AuNP core by using gold-catalyzed polymerization of alkynes.[91] Subsequently, the Au can be dissolved out of this structure without disrupting the overall size, shape, or binding capability of the DNA corona, making a "3D spacer" that connects PAEs into a lattice. These hollow particles are a key example of a design parameter that would not be achievable in either

atomic systems or close-packed colloidal lattices, thereby enabling the synthesis of non-close packed crystallographic symmetries (Section 3.3) and truly demonstrating the tailorability, diversity, and control afforded by DNA-programmed assembly.

PAEs have been synthesized on both the nanoscale (2 nm to 1,000 nm)[45,89,92] and microscale[93–95] with the same basic DNA design, and all follow the same design rules as particles in the ~10-50 nm core size regime[74,96] (Figure 3). The key rule that governs the crystallization of different PAE sizes is that the overall hydrodynamic radius of the PAE determines its binding behavior, not the core size alone.[69] However, at the nanoscale, the accessible size regimes are energetically limited to a "zone of crystallization" based on DNA length to NP diameter ratio.[96] Conversely, in PAEs constructed from particles at larger length scales (e.g. ~1-3 µm), the DNA strands are often significantly shorter than the particle diameter, meaning that the particle size ultimately dictates the range of accessible lattice parameters.[93]

A majority of the NP cores in demonstrated PAEs are spherical and isotropically functionalized with DNA, as these highly symmetric constructs are easier to synthesize. However, in an effort to add more complexity to the PAE core and mirror the ability of atoms to adopt directional binding as a function of valency, several different strategies of PAE construction have been developed. First, while early work in PAE synthesis revealed multiple routes to either patchy[26] or asymmetrically functionalized particles,[97] the particles synthesized with these methods have not yet been demonstrated to form ordered crystals, and breaking the symmetry of spherical building blocks remains a challenge. Nevertheless, by functionalizing specific sites on pseudo-spherical proteins with DNA, PAEs were synthesized with tunable and precise bond distributions where both the number and direction of DNA linkages were controlled.[98–101] Such constructs have been demonstrated to produce arrangements that are unachievable with isotropically functionalized spheres.[99,100] It is even possible to functionalize different sites on the same protein with orthogonal DNA sticky ends, thereby yielding Janus-type PAEs that assemble into 1D crystalline chains,[101] or complex

layered crystalline structures of PAEs that alternate in NP core identity (composition or size)[100] (Section 3.3). A second strategy to impart directional interactions between spherical particles involves trapping NPs within or at the vertices of anisotropic DNA origami constructs.[102–104] The 3D shapes of these structures dictate both the valency and possible binding directions of the overall construct, meaning that the shape of the contained spherical particle is separated from the factors that dictate lattice symmetry. This method enabled a non-close-packed diamond-type NP superlattice[102] and was later expounded upon using various DNA frameworks to achieve a breadth of crystalline symmetries.[103]

A separate strategy to control valency and directional binding in PAEs relies on isotropically functionalizing a non-spherical NP, such that the shaped core acts as scaffold whose local geometry enforces direction on the DNA binding groups.[105] This method is particularly promising given the wide array of synthetic protocols able to produce anisotropic NPs.[106–110] It was demonstrated that anisotropic NPs with flat faces tend to favor arrangements in which these flat faces are aligned parallel with one another in order to maximize DNA hybridization interactions, a concept understood as shape complementarity.[111] This anisotropic directing force drives self-complementary plate-like NPs to form 1D chains, rods to form 2D hexagonal lamellae, cubes to from 3D simple cubic (sc) lattices, etc.[111–113] Shape complementarity has also been extended to include binary co-crystals of different shapes, generating crystallographic arrangements that would not be possible with other NP crystallization schemes.[111,114,115] PAEs have also recently capitalized on a synthesis method that produces clusters of spherical PS particles with well-defined arrangements.[116] Given their high stability, the clusters can then be DNA-functionalized and used as a PAE core with complex shape. This strategy not only enables PAE "reactions" between two clusters akin to molecular reactions but also is shown to produce unique crystalline symmetries[89] enabled by the shape of the cluster.[117]

3.2. Programming Dynamic Assemblies *via* Controlled DNA Binding

DNA was originally conceptualized as the ideal binding moiety for a PAE due to its high information content and predictable nucleobase interactions. Indeed, DNA has proven its programmability through tunable complementarity, length, binding strength, flexibility, and even dynamic manipulability. Given the molecular purity of oligonucleotide synthesis and the high persistence length of double-stranded DNA (dsDNA), the lattice parameter of a PAE crystal can be linearly controlled based on the number of base pairs that constitute a PAE-PAE bond.[118] The binding strength between PAEs is mediated by DNA sticky end sequence, number of linkers added to a PAE, and the solution's salt concentration; thus, each of these variables can be used to tune the temperature at which crystallization occurs.[71] Bond strength can even be post-synthetically increased through the use of ruthenium coordination complexes,[119] ethidium bromide,[120] or silver ion intercalators.[121] While dsDNA is relatively stiff, the flexibility of DNA strands between PAEs can be independently tuned by incorporating ssDNA bases or polyethylene glycol "flexors" to effect crystallization ability and quality[122] or alter the entropy penalty associated with PAE bond formation, which can result in alterations to PAE superlattice structure.[123]

To a great extent, the DNA corona of a PAE dictates its binding characteristics in a manner analogous to how electron orbital shape and energy dictates atomic bond formation.[1,5,6,124] The characteristics of the DNA corona (complementarity,[69] directionality,[111] etc.) yield consistent crystallographic symmetries in PAEs similar to orbitals dictating the final arrangement of atoms within the unit cell. One of the foremost analogies between PAEs and atoms is that both exhibit a well-defined equilibrium bond length based on a balance of repulsion and attraction **(Figure 4)**. The interatomic distance between two atoms is often modeled by a Lennard-Jones potential[5,125,126] where there is an energetic minimum at a specific spacing balanced by the repulsive force of overlapping electron orbitals and the attractive force of atomic binding. Similarly, it has been shown both experimentally and through computational modeling that the interparticle spacing of binding PAEs reach an equilibrium

length due to a balance of the electrostatic repulsive force between negatively charged DNA coronae and the enthalpic attractive force of maximizing DNA hybridizations.[127] Both forces can thus be modified through changing salt concentration (electrostatic shielding)[127,128] and changing sticky end binding strength, respectively.

Further investigation concerning DNA's behavior in different solution environments allows for dynamic manipulation of the DNA corona and thereby the PAE lattice. Adjusting from a phosphate buffered saline solution to ethanol causes reversible, dynamic changes in lattice parameter due to adjustments in the local dielectric constant and thus interparticle repulsion.[129] Additionally, the addition of free water-soluble polymer to the solution causes lattices with significant regions of unpaired (and thus more flexible) ssDNA in their linkers to compress due to an increased osmotic pressure.[130] The incorporation of "i-motif" sections into the DNA linker strands allows for the PAE lattices to be adjusted as a function of solution pH, as i-motifs exhibit condensed structures at low pH and extended conformations at high pH.[131] Unfortunately, these adjustments are often small in magnitude given that the stability of a DNA double helix is restricted to a small set of solution conditions and fairly radical changes in solvent environment tend to destabilize dsDNA.[132–134]

However, the programmability of DNA base-pair sequences can induce more dramatic manipulation of PAE lattices by tailoring which bases along a DNA linker hybridize with one another. Specifically, the inclusion of DNA "hairpin" structures in the linker sections of PAEs was initially shown to reversibly and precisely toggle the lattice parameter of PAE lattices upon addition of DNA sequences to open and close the hairpin.[135,136] This motif was further developed to enable toggling between "activated" and "deactivated" states, thereby affecting both the number and nucleobase sequence of the sticky ends expressed on each particle. As a result, particle stoichiometry within a lattice, the ratio of the number of linkers contained on each PAE in a binary structure, and which PAEs were able to form bonds with one another could be reversibly altered, enabling the ability to dynamically toggle a lattice between different

crystallographic symmetries.[137] It is worth noting that, although each different state of a hairpin-containing PAE mimics atomic crystallization behavior in the manners discussed here, the ability to switch this binding behavior independently of elemental composition is not possible in atomic systems. While the programmability and complexity of DNA structure allows for an individual particle to exist in multiple forms that possess distinct binding behavior, there is no way to "transmute" an individual atom to change its inherent bonding characteristics without changing its electronic structure. As a result, these hairpin-containing particles are a key example of how PAEs are more than simple nanoscale artificial atoms.

3.3. Programming Local Coordination within a PAE Lattice

As a result of the elucidation of the PAE crystallization design rules[96] and the development of PAEs of various shapes, sizes, and binding directionality (Section 3.1), a vast library of lattice symmetries has been realized for PAE crystals **(Figure 5)**.[138] While the first unit cells that were synthesized formed relatively simple fcc and bcc symmetries, the engineering of superlattice crystallographic arrangements has since broadened to include binary structures isostructural to cesium chloride (CsCl), aluminum diboride (AlB$_2$), chromium silicide (Cr$_3$Si), and an AB$_6$ structure that has no atomic analogue but is isostructural to the alkali-fullerene complex Cs$_6$C$_{60}$.[74,93] Importantly, mirroring binary mixtures of atoms, an entire binary phase diagram was elucidated where PAEs of differing relative sizes and amounts of linkers were found to maximize the DNA hybridization between nearest complementary neighbors and determine the energetically most stable unit cell.[74] These initial phase maps have since been refined using theoretical modeling[139,140] and extended to include stoichiometric phase behavior.[74,141] Unachievable in binary atomic unit cells, the "hollow" PAEs (Section 3.1) enabled the selective omission of one constituent, effectively creating sc lattices from bcc, graphite-type (omit A) or simple hexagonal (omit B) structures from AlB$_2$, and bcc (omit B) or 'lattice X' (omit A) – a crystallographic unit cell unique to only this system – from AB$_6$ symmetries.[91]

More complex functionalization of PAEs with both two different sets of linkers (one with self-complementary sticky ends and the other with sticky ends complementary to a second PAE) was shown to enable both sc and sodium chloride (NaCl) unit cells.[74] This same strategy of using multiple and orthogonally programmable DNA binding interactions was later used to create ternary lattices. This method involved first assembling a binary "parent" lattice using one set of complementary DNA sticky end interactions and later infiltrating this lattice with a third type of PAE capable of weakly binding to both parent PAEs, precisely designed so that it filled in the interstitial holes of the parent structure.[142] These ternary systems resulted in perovskite-type ABC_3 unit cells, as well as several unit cells without known atomic analogues (ABC_{12}, A_2B_3, AB_4), making these lattices the first NP-based crystal structures that were rationally designed *prior* to synthesis.

While the predominant driving force that dictated the thermodynamically favorable lattice structure for a given set of PAEs was initially discovered to be almost entirely an enthalpic maximization of DNA binding, it was later found that entropic effects could be increased with flexible DNA linkers, thereby inducing self-complementary PAEs to form a bcc lattice even though this structure represents a lower packing density than the prior fcc structures that had been obtained in unary systems.[123] Making the core-core interactions appreciable in scale, one study found the binary phase isostructural to sodium-thallium (NaTl).[92] Additionally, it was discovered that higher energy unit cells could be synthesized in a kinetically trapped state under the correct conditions (e.g. hexagonal close packed (hcp) lattices form as a kinetic structure for PAEs whose thermodynamically preferred phase is fcc).[74] Another unique phase, isostructural with thorium phosphide (Th_3P_4), was isolated by changing the binding motif to one with increased "bond order" (achieved by using branching DNA strands where each linker terminated in multiple sticky ends).[143] Finally, the PAEs with programmed valency and directional binding as a result of anisotropic core shape or surface functionalization (Section 3.1) have exhibited several unique lattice arrangements not currently realized in PAEs with

isotropic binding, namely 1D and 2D crystals,[101,104,112,113] body-centered tetragonal (bct) unit cells,[103,115] layered structures,[100] the Laves phase isostructural to dicopper magnesium (MgCu$_2$),[89] and even diamond symmetry.[102] As these more complex phases indicate, further experimental and theoretical investigations are required to garner a full understanding of the multiple different forces that are important in dictating PAE assembly. This review proposes the following perspective to serve as inspiration for future exploration of the DNA-grafted NP field: approaching PAE crystallization through the lens of atomic crystallization can offer insight and explanation to much of the complexity within colloidal NP crystallization.

4. Directly Analogizing Colloidal PAE Assembly to Atomic Crystallization

The major advantages of the PAE system in producing NP superlattices are the diversity of structures that can be synthesized and the programmability that allows for researchers to specifically dictate the lattice parameters and symmetries of the material being made. Importantly, this programmability stems from not only the predictability of DNA hybridization but also from the fact that the crystallization of PAEs can be readily explained using the wealth of knowledge that has been developed from studying atomic crystals. In contrast to early work using colloids as "artificial atoms" (Section 1), the formation of PAE crystals mediated by DNA binding uses localized concentrations of sticky ends that can be analogized to atomic binding *via* localized electron orbitals. This results in lattice formation that follows fundamentally similar nucleation and growth dynamics as observed in atomic systems, as well as classical atomic materials science principals such as surface faceting, defect structures, and epitaxial deposition.

Many of these analogies were discovered by using atomic crystallization behavior as inspiration for hypotheses to investigate new PAE behavior, and the conclusions found in those studies were often explained by viewing them through the lens of known atomic behavior. However, unlike atoms whose binding characteristics are innately tied their atomic identity, modular PAEs can independently adjust individual variables to further investigate the observed

phenomena in a way that is unachievable in atomic crystals, enabling more complex structure-property relationships to be developed (Section 5.1).

4.1. Nucleation and Growth Dynamics of PAE Lattices

Due to the similarities in binding behavior between atoms and PAEs, their crystallization dynamics are expected to follow analogous behaviors. Indeed, the "melting" temperature (T_m) of PAEs is several degrees higher than the "crystallization" temperature, as measured by UV-Vis spectroscopy.[144] This is due to a phenomena called undercooling, a form of super saturation commonly observed in atomic metals and even water.[1,145,146] There is a zone of temperatures below T_m where the driving force for nucleation is so low that crystals do not form in appreciable amounts; within this region, the free PAEs are metastable. Interestingly, the metastable zone width in the PAE system was found to be dependent on the valency of the PAE used.[144] The higher number of nearest neighbors the particle could support, the higher the energy barrier for nucleation, and therefore, the higher degree of undercooling required to induce nucleation. This is an example of a variable trait that cannot be independently studied in atomic systems where the valency of the atom is inherently tied to its identity.[5] Thus, the effect of nearest neighbor number on nucleation barrier in atomic crystals cannot be investigated without changing the constituent components and thereby introducing more variables into the nucleation behavior but, conversely, can be studied with PAEs.

A more thorough investigation of PAEs' crystallization behavior has been done with *in situ* structural analysis of crystallite size and quality during nucleation and growth. These studies demonstrated that PAEs display classic nucleation and growth behavior that has been comprehensively explained for atomic solids, where small clusters form, reorganize into crystalline nuclei of a critical stable radius, then grow in domain size as a function of solution temperature.[147] However, these dynamics can be easily tuned by adjusting PAE characteristics (sticky end sequence, number of linkers, and salt concentration)[71] whereas atoms' behaviors are generally dictated by the valencies and bond strengths inherent to their element. Based on

optical observations, it has been hypothesized that PAE crystal formation from an initial amorphous aggregate follows an "Ostwald ripening" behavior common to atomic crystallites where atoms migrate from small crystals to large crystals due to a size-dependent difference in melting temperature.[62] Molecular dynamics simulations, however, have shown behavior more akin to oriented attachment/rearrangement,[148] indicating the potential for further investigation into this complex behavior (Section 5.2).

PAE crystallization has also been experimentally shown to exhibit more complex crystallization phenomena, such as the classic time-temperature-transformation (TTT) behavior of atomic materials. TTT diagrams have a distinctive C-shape as a function of the undercooling temperature where a maximum rate of crystallization occurs at a specific temperature due to a balance of nucleation (faster at low temperatures due to larger undercooling and energetic driving force) and growth speeds (faster at high temperatures due to more thermal energy).[1] This behavior was characterized first in nanoscale PAEs using *in situ* small angle X-ray (SAXS) measurements[71] and later directly observed and mapped through optical, *in situ* imaging of micron-sized PAEs (**Figure 6A**).[93]

When a batch of PAEs is slowly cooled such that nucleation and growth occurs under equilibrium conditions, the crystallites adopt thermodynamic Wulff constructions with a controlled and predictable habit (overall faceted shape).[149] Behaving exactly like atomic crystals, the resultant shape is dominated by the slowest growing planes of the lattice, resulting in a Wulff polyhedron whose shape is characteristic to the crystallographic unit cell and planar energies.[1,150] Single PAE crystallites displaying faceting consistent with the Wulff construction have been observed for the bcc, CsCl,[149] and AlB_2[151] symmetries and for several anisotropic PAE systems[152] (Figure 6B). The nearly perfect crystallites only exhibited minor defects of "adatoms," ledges, kinks, and terraces on the planar faces,[149,151] which are also commonly observed in growing atomic crystals. Finding inspiration from chemical engineering studies in existing crystal processing techniques used to sharpen size distributions of grown

atomic crystals, recent work in the batch crystallization of PAE crystallites selectively removed those beyond a critical size with gravity to halt their growth and increase single-crystal size uniformity.[153] The process utilized a "batch crystallizer" solution of free PAEs placed above an immiscible, more dense liquid that would not allow free PAEs to disperse within it. Once crystals nucleated and grew to a critical size, gravitational forces were enough to sediment the PAE crystallites into the liquid without free particles, arresting their growth. Each of the investigations discussed in this section demonstrate that the strongest parallels between atoms and PAEs exist in this area of crystallization dynamics, allowing researchers to efficiently and effectively implement and apply the strategies used in atomic systems to control aspects of PAE crystallite size, shape, faceting, etc.

4.2. Interactions at Interfaces and Epitaxy

Behavior at a substrate surface represents an active area of research in both atomic and PAE systems due to the unique properties that arise from interfacial interactions, as well as potential applications that thin film materials enable.[154,155] In this regard, a number of studies have explored the thermodynamics and kinetics of PAE adsorption to a functionalized surface. For example, when PAE attachment onto a surface was restricted to lithographically defined gold "landing pads," adsorption that satisfies the assumptions of the atomic Langmuir model was observed.[156] Further restricting the free motion of PAEs by forcing movement through PMMA wells to reach interfacial attachment sites, PAEs kinetically followed Fick's classical law of diffusion (akin to atoms or molecules diffusing through pores)[157] and were organized into complex architectures through this strategy of template-confinement.[158] The interfacial binding strength and surface mobility of substrate-bound PAEs were found to be dependent on both PAE design features (e.g. sticky end length)[159] and substrate design features (e.g. areal DNA density)[160] with degrees of programmability difficult to attain in atomic adsorption. However, these studies were primarily limited to individual PAEs, small clusters, or monolayers.

Ultimately, the first example of bulk PAE crystallization at a surface used a method analogous to atomic layer deposition, where PAE thin films were synthesized using layer-by-layer deposition of complementary PAEs onto a flat DNA-functionalized substrate.[161] This proof-of-concept work demonstrated that the orientation of the thin film grains could be predictably controlled by the functionalization of the substrate with either one or both types of complementary sticky ends **(Figure 7A)**. This preferential alignment of PAE orientation is directly mirrored in atomic thin films where grains of certain alignments relative to the substrate are energetically stabilized by it and thus dominate in the thermodynamic product.[162,163] In cases where this stabilization is extremely favorable, the depositing material will adopt the crystallographic arrangement and even lattice parameter of the substrate material in a process known as epitaxy.[164]

Recent advances have built upon the early work that used unpatterned surfaces by developing a platform that mimics the process of atomic epitaxy at the nanoscale with PAEs. Epitaxial deposition was demonstrated by first using lithographic patterning to produce a template of nanodots, where the shape of the nanodots was consistent with the size and shape of the deposited PAEs' NP cores, and the arrangement of the nanodots mimicked a particular crystallographic plane of the PAE lattice.[165] Following DNA functionalization of the nanodots and subsequent deposition of complementary PAEs, a layer of PAEs formed that matched the underlying patterned plane. By tailoring the structure of the lithographically defined patterning, monolayers were epitaxially grown to match the {100}, {110}, and {111} crystal planes of a bcc superlattice.[165] Later work demonstrated that subsequent rounds of deposition enabled the synthesis of a multilayer, millimeter-sized single-crystal (Figure 7B).[166] This proxy platform was then used to investigate the alleviation of strain due to lattice mismatch in the PAE thin films by patterning nanodots with periodicities inconsistent with the equilibrium, bulk PAE lattice parameter.[167] PAEs exhibited similar strain alleviation mechanisms as are hypothesized to occur in atomic systems,[168] including elastic relaxation and defect formation (vacancies and

misfit dislocations).[167] This work also highlights a conceptual advance in controlling PAE microscale structure through combining top-down lithographic templating and bottom-up PAE self-assembly. With such a template, the overall shape of the crystallite is dictated by a set of arbitrary boundary conditions, and its size is theoretically unlimited beyond the conditions that limit the size of the pattern that can be lithographically fabricated.[166]

5. Future Areas of Investigation for PAE Crystallization

5.1. Using PAEs as a Proxy System to Study Atomic Crystallization

As more analogies between atomic crystallization and PAE crystallization are elucidated, the atomic scale continually provides concepts and knowledge that can be explored at the nanoscale using PAEs. In turn, PAEs could potentially provide a nanoscale platform through which specific crystallization behaviors that are challenging to directly study at the atomic scale could be investigated (**Figure 8**). This section will elucidate potential areas of investigation in which the programmability of DNA-coated NP assembly has not yet been fully realized as a means to understand basic crystallization phenomena, but in which there exists significant potential for scientific discovery.

Historically, proxy systems have precedence in elucidating atomic behavior before direct analytical techniques are available. For instance, "bubble rafts" were used to observe grain boundary formation,[169] providing the first experimental evidence for behavior such as plastic deformation *via* slip and impurity segregation at the grain boundary.[170,171] The main advantage of the bubble raft proxy system is that bubble rafts can be observed with the naked eye, while atomic scale resolution was only developed decades later.[172] On the same principle, PAEs as analogs for atomic systems can be readily imaged with micron scale or even nanoscale resolution, allowing for optical and electron microscopy techniques to monitor the crystallization processes with real-space imaging techniques.[93,173,174] Furthermore, the properties of a PAE (binding characteristics, size, relative softness, etc.) are precisely programmable and tunable (Section 3), whereas an atom's characteristics are dictated by its

identity. Utilizing atoms as building blocks, it is difficult to independently adjust variables like size and binding strength without simultaneously changing characteristics such as binding direction or electronic properties.[124] Using PAEs as a proxy system could enable the independent investigation of the effects of specific variables on complex, atomic phenomena. One potential area of investigation is why certain systems undergo surface diffusion *via* atom exchange mechanisms as opposed to adatom hopping mechanisms.[175] Current theories include effects from tensile surface stresses, surface relaxation about the adatoms, or increased stability from surface-adatom interactions during coordinated exchange.[176] Using PAEs as a proxy system, in which the effects of each of these parameters may be isolated by separately programming adatom-surface, surface-surface, and surface-bulk interactions (Section 3.2), could provide more controlled empirical datasets relative to that provided by existing atomic systems and facilitate the development of a theoretical framework behind these distinct mechanisms.

The PAE building block provides a platform for structure control across many length scales, including the elemental composition of the NP cores, the nanoscale size and shape of the particle and DNA linkers (Section 3.1), the coordination environment of the particle within a crystallographic unit cell (Section 3.3), and potentially the lattice superstructure (crystallite habits, orientations, and defects) (Section 4). However, most of the potential and hypothesized applications of PAEs as a proxy system to study analogous atomic crystallization behaviors and as a unique materials synthon are just beginning to be realized. An ever-growing understanding of the PAE construct and its colloidal assembly behavior is necessary to develop both analogies to atomic behavior as well advance the field of colloidal interactions in general. Thus, this review encourages both experimental and theoretical research that facilitate in understanding the complexities of dictating structure in PAE assemblies, in particular the development of new analytical tools and imaging techniques.[173,174]

5.2. Development of New Tools and Techniques to Probe PAE Assembly

Major breakthroughs in materials design are often preceded by the invention of new diagnostic tools or instrumental measurement techniques, as these allow for exploration of previously unanswerable research questions. As understanding of the strengths and limitations of analogizing PAE assembly to atomic crystallization are elucidated, many of the hypotheses that could be probed will require advancements in characterization tools to fully explore these comparisons. A key area of investigation for PAE crystallization is therefore the development of new tools and techniques that allow for complete understanding of PAE assembly behavior. For atomic systems, *in situ* imaging of chemical reactions has only been achieved using sophisticated non-contact atomic force microscopy with a single carbon monoxide molecule tip.[177] However, the PAE proxy system occurs at significantly different size, time, and energy scales that make PAE assembly potentially much easier to directly observe and characterize *in situ*.[93,178] If the studies into the complex factors that control PAE assembly continue to show strong correlation to atomic crystal formation (Section 4), it is reasonable to hypothesize that the direct observation of these phenomena could lead to generalizable insights into not just the thermodynamics of crystallization but also the pathways by which both colloidal and atomic crystals form. Nevertheless, the predominant method for monitoring nanoscale PAE assembly *in situ* still relies on reciprocal space techniques such as X-ray scattering. While SAXS has allowed for real-time examination of crystal formation in nanoscale PAEs,[147] this method is indirect and provides information solely about the bulk structure of the lattices being formed.[179] At larger length scales, micron-sized PAEs have been observed using optical microscopy, which has already afforded a wealth of information on material structure during the crystal growth process.[93] Nevertheless, these PAEs are typically only examined in pseudo-2D architectures that are significantly affected by gravitational forces, meaning that their behavior may not entirely mimic atomic crystal formation.

In principle, recent advances in solution phase electron microscopy[178] could be used to examine PAE assembly at the nanoscale—indeed, some examples of *in situ* imaging NP

crystallization (using non-PAE architectures) have already been developed,[173,174] indicating that this method has significant potential for examining PAE behavior. The major challenge for such a technique is in producing an *in situ*, solution phase electron microscopy platform with the necessary resolution that uses non-damaging levels of radiation to the PAE construct. However, the establishment of such a technique would provide significant benefit for the use of PAEs as atomic proxy systems (Section 5.1), as it could allow for imaging of crystallization behaviors that would be challenging or impossible to observe in atomic crystals.

Importantly, development of these *in situ* techniques would further enable the ability to investigate atomic systems through a PAE proxy by taking advantage of the independently programmable design handles to isolate the effects of each individual PAE characteristic. For example, while some techniques exist to image behavior such as defect diffusion or surface diffusion in atomic systems,[180–182] a PAE proxy system would allow for investigation into changing one parameter, such as bond energy, without altering any other properties like building block size or bond directions. Additionally, *in situ* microscopy would enable direct observation of phenomena like grain formation and grain growth mechanisms which have been hypothesized for atomic grains but prove incredibly difficult to track at the level of each individual atom.[183–185] Ultimately, such a technological advance would allow for the use of PAEs to investigate any number of crystallization mechanisms including TTT behavior in nanoscale PAEs, Ostwald ripening versus oriented reattachment of crystallites, defect formation, grain boundary diffusion, plastic deformation, and crystal growth both homogenously and heterogeneously at interfaces. Furthermore, this more advanced observation of PAE assembly would enable a deeper understanding to the complex combination of forces that contribute to colloidal behavior beyond those already analogized in the "atom equivalent" framework. We would note that, in the context of nanoscale PAEs, the direct imaging of crystal formation remains an underinvestigated area. Thus, while the strong analogies to atomic crystallization indicate that the projected benefit from such studies would be large, it remains

to be seen exactly how much information gained from such systems can be directly generalized to atomic crystallization. We would therefore encourage the community to continue to develop characterization tools to achieve this goal.

5.3. Arbitrary Control over Superlattice Habit

In addition to a stronger understanding of the dynamics of individual building blocks, a second major goal for PAE superstructure control is the ability to arbitrarily control PAE crystallite habit (size and shape). Recently, single-crystal PAE architectures have been used as individual optical devices in geometrically sensitive applications, reliant on their well-defined, thermodynamic Wulff polyhedron structure.[186–188] Furthermore, theoretical work indicates that AuNP superlattices of precisely defined shapes exhibit unique optical responses.[189,190] However, the shape of the currently accessible Wulff crystals[149,151,152] is inherently dictated by the crystallographic symmetry of the corresponding unit cell and cannot be arbitrarily manipulated. If successful in dictating PAE crystallite size and shape, such a structure-defining strategy would advance the understanding of colloidal crystallization and broaden the realm of applications available to NP-based crystallites.

In atomic systems, multiple mechanisms have been explored as a means of controlling crystal habit,[191] and many of these have yet to be examined in PAE superlattices, indicating a wide area of potential research opportunities. For example, limited tuning of superlattice shape could theoretically be achieved by nucleating crystals at a DNA-functionalized surface, possibly allowing for tunable Winterbottom constructions that effectively truncate the thermodynamically preferred Wulff polyhedra at specific lattice planes, taking advantage of DNA's programmability to tune substrate-PAE interactions.[192,193] Extending this strategy of imposing boundary conditions on PAE crystallite growth, the Summertop formalism (where nucleation and growth are restricted by multiple interfaces)[194] could also be investigated by assembling PAEs at surfaces with concave or convex shapes. Alternatively, just as metal NPs of varying shapes have been synthesized through the introduction of facet capping agents during

nucleation and growth,[108,110,195,196] it may be possible to manipulate PAE superlattice crystal shape using nanoscale "capping" constructs. Each of these hypotheses to control PAE crystal habit utilizes an atomic mechanism as inspiration. However, none of the methods has been explored yet, and no analogous means of using these mechanisms to control PAE lattice habit has been developed to date.

In atomic systems, the synthesis of heterocrystals with disparate material properties allow for the fabrication of devices, such as transistors, enabled by junctions of semiconductors with different band structures (e.g. non-uniform composition or doping profiles).[197–199] Analogously, the development of crystals that possess a singular overall crystal structure but different PAE compositions at different points along the lattice would yield spatially variant properties within a PAE material, enabling the creation of highly complex NP-based devices if the variance is well-understood and programmable. It is important to note that such a structure could be achieved due to the fact that the packing of PAEs within a lattice is dictated by the overall hydrodynamic radius of the building blocks, and the identities of the NP cores can be tailored independently of this value (Section 3).[74] As a result, multiple different PAEs could, in principle, be used to form a single crystal structure, even if their NP cores were widely varied in size or elemental composition.[74,77,78,82,86,200]

Recently, preliminary work has been done to extend spatial control over PAEs at a surface by templating the deposition of PAE films using top-down lithography methods (Section 4.2). Strategies include using site-specific e-beam irradiation to damage a DNA-functionalized interface prior to deposition of a PAE monolayer resulting in NP size segregation,[160] depositing PAEs onto lithographically defined gold "landing pads" or into PMMA wells,[156–158] and epitaxial deposition on arbitrarily shaped arrays of gold nanodots.[166,167] Future work may be done to investigate post-processing techniques to manipulate the PAE material after assembly. For example, lithographic ablation could potentially be used to controllably remove sections of the PAE aggregate without altering or

damaging the other regions of the superstructure. The development of such high fidelity, high precision lithographic techniques would enable the construction of nanomaterial devices from PAE materials, taking full advantage of the properties nanostructured architectures provide. It is important to note that much of this work is still at the stage of simply developing the prerequisite tool-set needed to make such complicated structures. Regardless, pairing the programmability of DNA-encoded assembly with sophisticated lithographic patterning techniques could potentially enable hierarchical structures with design features across multiple length scales; similar types of structures that have been fabricated *via* lithography alone have shown promise for developing materials with multiple unique physical properties.[201–204] The advantage of the PAE system would be to improve the resolution,[118] complexity,[74] or stimuli responsiveness[131,137] of such systems.

5.4. Expanding the Properties of Nanostructured Materials

In NP-based materials, properties are garnered through the collective properties of the constituent composite materials (i.e. PAE core composition, Section 3.1),[110,205,206] but, more importantly, emergent properties can arise from an ordered, nanoscale structure,[207] which PAEs are able to provide with exquisite programmability (Section 3.3). While many of the properties that will be discussed in this subsection have only been proposed and not yet realized, it is important to note that PAEs do indeed provide a unique platform for studying structure-property relationships. Thus, the key advantage of PAEs in developing new structures is not necessarily in providing access to materials for commercial or industrial applications but rather in better understanding how material organization across multiple length scales can be used to tune such physical and chemical characteristics. As specific examples, this subsection explores the impacts of structure on the optical, electrical, and mechanical properties of NP-based materials.

At the atomic scale, optical properties are dictated by interactions between photons and electrons in the material **(Figure 9)**.[208,209] However, in "photonic" materials with periodic

structures at length scales comparable to the wavelength of visible light, diffraction from superlattice subunits can be used to design interference conditions to further manipulate light in the material.[208,210–212] A common example of this is a phenomenon known as "structural color," in which a band of light exhibits destructive interference within the material and is, therefore, reflected rather than transmitted. The result is a bulk material color not exhibited in a non-assembled or randomly positioned set of NP subunits.[213–215] Specifically, PAEs have demonstrated structural color due to index contrast between slip planes, causing reflection of specific wavelengths.[216] However, a thorough investigation into the effects of PAE design variables (e.g. lattice parameter, NP core shape, etc.) on the resulting color and further optical properties of NP assemblies still remains an underdeveloped area of research.

Electrical behavior in atomic systems is governed by electron-lattice interactions within the material,[217,218] but materials with coupled capacitive and inductive subunits can be used to design collective excitation behaviors (Figure 9).[219–221] Macro-scale antenna arrays have utilized these concepts to manipulate electromagnetic fields in exotic ways, such as the split-ring resonator arrays to generate negative refractive-index surfaces enabling stealth planes to remain undetected by radar.[219] By fabricating similar coupled structures at the much smaller nanoscale, it would be possible to extend this cloaking behavior into the visible.[222] However, conventional, top-down lithographic techniques capable of fabricating the nanoscale features required to manipulate wavelengths of light in the visible spectrum are impractical methods to generate large, 3D patterns.[223,224] This inherent tradeoff between resolution and bulk synthesis restricts these unique materials to either limited-size applications or the manipulation of low-frequency electromagnetic waves, such as radio waves. Conversely, PAEs offer a programmable, bottom-up synthesis approach to create and study 3D bulk materials with well-defined nanostructure, promising an expansion of light-manipulating applications for NP-based materials.

In atomic systems, phonons are responsible for the transport of sound and heat through a material due to atomic vibrations (Figure 9).[217,225] Previous work has demonstrated that NPs embedded into a substrate can modify the behavior of these phonons by either modifying the interfacial behavior of the embedded matrix[226] or by causing phonons to scatter.[227] As with photonic and electronic structural properties, designing a PAE system with interfering mechanical modes, or coupled mechanical oscillations, could potentially allow for structural control over simple mechanical properties (e.g. propagation of heat and sound).[228] More sophisticated structures, such as auxetic composites at the macroscale,[229] have demonstrated exotic properties that are specifically enabled by collective behavior (e.g. negative Poisson ratio[230]). Because these behaviors are dictated solely as a function of the overall organization of structural features and not length scale, nanoscale equivalents are hypothesized to be achievable with PAEs due to their exquisite control over hierarchical organization; however, this would require further investigation into the mechanical behavior of PAE lattices, as well as techniques to probe PAE structural response to mechanical stimuli.

While the potential for PAE-based materials with exotic properties is enormous, many of these applications require NPs with specific elemental compositions. However, not all compositions, sizes, and shapes of NPs that can be synthesized have been demonstrated as templates for PAEs as yet (Section 3.1). The major challenge limiting the number of particle compositions that can be examined in PAE crystallization is that new attachment chemistries will be required to functionalize a dense monolayer of DNA on those materials. While there have been some attempts at creating a generalizable attachment chemistry for DNA to NPs of arbitrary composition,[77] this methodology has not been widely adopted due to the challenging synthetic protocol and limited yields. Additionally, the current crystallographic symmetries available to PAEs almost exclusively rely on isotropic particles, and different particle valencies are largely imparted by the use of different NP core shapes (Section 3.3);[112] this is in direct contrast to the atomic valencies that give rise to complicated and low symmetry lattices.[5,196]

In theory, PAEs with greater control over the directions of their bonds could be realized with the development of anisotropically functionalized particles. Simulations reveal that such "patchy" PAEs with specific binding sites across their surfaces would have unique self-assembly behavior,[231] but the currently synthesizable patchy particles have yet to produce crystalline materials with long-range order.[26] However, if successful, anisotropic control over assembly could enable creation of exotic analogs to atomic symmetries including quasicrystals,[232] chiral lattices,[233] or high-entropy alloys.[234] Research developments in chemistry will therefore be required to access the full programmable potential of the PAE building block.

In addition to limitations in accessible core compositions, one of the major inherent limitations in the utility of PAE-based materials synthesis is that DNA duplexes exhibit limited stability in different environments,[127,129,133,134] and thus, PAE lattices are not readily usable for many different devices or applications. Some techniques have been developed to increase the stability of the PAE system after assembly, such as incorporation of intercalating elements to increase the DNA binding strength[119,120] or selective nucleation of materials such as silica[235] or silver[121] in the vicinity of the PAE crystals, embedding them into stable states that can be removed from solution. Modifications to the DNA linkers (Section 3.2) enable further control of the material properties of the PAE system, such as the dynamic responsivity,[131] stability in varying environments,[129] Young's modulus,[235] or conductivity.[121] However, the physical and chemical limitations of DNA still inhibit transference of PAEs to a wide array of conditions.

As mentioned at the beginning of this section, the key advantage of PAEs is in the development of structure-property relationships that could later be explored in a more diverse set of building blocks that are not necessarily based on DNA-programmed assembly. As a result, much of the PAE work highlighted in this review provides a blueprint for such materials, allowing PAEs to serve as inspiration for future work and to aid the development of future building blocks. If a suitable replacement for DNA that possesses many of the characteristics

that enable PAE assembly (programmable binding interactions, controlled length, etc.) were developed, much of the work elucidated in this review could be translated to a significantly greater range of material designs. An example would be to replace the DNA with different polymeric analogues, thereby enabling control as a function of both the NP core and the ligands that bind the particles into a lattice. Recently, the first example of such a broadly tunable NP structure has been developed, dubbed the "nanocomposite tecton" (NCT).[21] NP superlattice synthesis with NCTs has demonstrated that many of the concepts developed in the PAE system can apply to a generalized NP building block thus allowing the significant amount of information that has been outlined in this review to be translated to potentially a significantly wider array of materials. As a proof of concept, initial work on NCTs used poly(styrene) ligands rather than duplexed DNA, where a complementary hydrogen bonding motif at the ends of the poly(styrene) chains enabled multivalent binding interactions between particles. Like the PAE system, the NCTs exhibit selective particle-particle bonding that allows for the assembly of superlattice structures with independently tunable particle size, interparticle spacing, and crystallographic symmetries. However, unlike the PAE system, NCTs use no expensive biological components and are stable in nonpolar solvents. This work to replace DNA with a wider range of materials greatly expands the design space of accessible material properties, including new mechanical, optical, thermal, or chemical properties.

6. Conclusion

This review highlights the development and impacts of the "programmable atom equivalent" building block constructed from DNA-grafted NPs. Specifically, how these unique colloids mirror atomic behavior can be used as the framework of an effective strategy for the rational synthesis of hierarchical materials. DNA is arguably the most programmable directing ligand available for NP self-assembly methods due to its precise and tunable Watson-Crick base-pair hybridization. Thus, the architecture of a PAE that expresses a discrete nanoscale orientation of DNA "sticky ends" enables multivalent, cooperative binding behavior that can

be used to generate crystalline arrangements of NPs that maximize DNA hybridization interactions. Importantly, the programmability and versatility in the binding capabilities of the PAE construct is derived independently from its modular core (size, shape, and composition), allowing for this synthon to be used to synthesize multiple different materials using a single assembly strategy. Moreover, because PAEs mirror many aspects of atomic binding behavior, the principles that have been extensively examined by chemists and materials scientists can be used to explain PAE crystallization, further enhancing their use in a programmable manner. Nevertheless, while a significant amount of research has been done to begin the process of fully drawing a correlation between PAE assembly and atomic crystallization, to fully understand and utilize the PAE platform further investigation into the assembly kinetics, arbitrary control over the size and shape of the crystallites, and creation of spatial variance is required. Such research will enable both the synthesis of designer materials, as well as the use of PAEs as an atomic proxy system where behaviors that are difficult to directly observe at angstrom length scales can be more easily characterized at the nanoscale. A full understanding of the assembly process of PAEs based on the framework described in this review will therefore enable a new era of materials synthesis demonstrating that the "programmable atom equivalent" moniker is indeed an appropriate label for these unique nanoscale building blocks.

Received: ((will be filled in by the editorial staff))
Revised: ((will be filled in by the editorial staff))
Published online: ((will be filled in by the editorial staff))

References

[1]   W. D. Callister, D. G. Rethwisch, *Materials Science and Engineering: An Introduction*, John Wiley & Sons, Hoboken, NJ, **2010**.

[2]   W. F. Smith, J. Hashemi, *Foundations of Materials Science and Engineering*, McGraw-Hill, **2011**.

[3]   R. T. Sanderson, *Chemical Periodicity*, Reinhold Pub. Corp., New York, **1960**.

[4]   W. M. Haynes, *CRC Handbook of Chemistry and Physics*, CRC Press, **2016**.

[5]   S. S. Zumdahl, D. J. DeCoste, *Chemical Principles*, Cengage Learning, **2012**.

[6]   L. Pauling, *J. Am. Chem. Soc.* **1929**, *51*, 1010.

[7]   J. W. Mullin, *Crystallization*, Elsevier, **2001**.

[8]   A. Lewis, M. Seckler, H. Kramer, G. van Rosmalen, *Industrial Crystallization: Fundamentals and Applications*, Cambridge University Press, **2015**.

[9]   A. G. Jones, *Crystallization Process Systems*, Elsevier, **2002**.

[10]   W. Caseri, *Macromol. Rapid Commun.* **2000**, *21*, 705.

[11]   A. Nasir, A. Kausar, A. Younus, *Polym.-Plast. Technol. Eng.* **2015**, *54*, 325.

[12]   A. N. Shipway, E. Katz, I. Willner, *ChemPhysChem* **2000**, *1*, 18.

[13]   S. H. Cole, E. A. Monroe, *J. Appl. Phys.* **1967**, *38*, 1872.

[14]   A. Van Blaaderen, R. Ruel, P. Wiltzius, *Nature* **1997**, *385*, 321.

[15]   M. E. Leunissen, C. G. Christova, A.-P. Hynninen, C. P. Royall, A. I. Campbell, A. Imhof, M. Dijkstra, R. van Roij, A. van Blaaderen, *Nature* **2005**, *437*, 235.

[16]   E. V. Shevchenko, D. V. Talapin, N. A. Kotov, S. O'Brien, C. B. Murray, *Nature* **2006**, *439*, 55.

[17]   X. Ye, C. Zhu, P. Ercius, S. N. Raja, B. He, M. R. Jones, M. R. Hauwiller, Y. Liu, T. Xu, A. P. Alivisatos, *Nat. Commun.* **2015**, *6*, 10052.

[18]   A. M. Kalsin, M. Fialkowski, M. Paszewski, S. K. Smoukov, K. J. M. Bishop, B. A. Grzybowski, *Science* **2006**, *312*, 420.

[19]   K. Heo, C. Miesch, T. Emrick, R. C. Hayward, *Nano Lett.* **2013**, *13*, 5297.

[20]   C. A. Mirkin, R. L. Letsinger, R. C. Mucic, J. J. Storhoff, *Nature* **1996**, *382*, 607.

[21]   J. Zhang, P. J. Santos, P. A. Gabrys, S. Lee, C. Liu, R. J. Macfarlane, *J. Am. Chem. Soc.* **2016**, *138*, 16228.

[22]   C. P. Collier, T. Vossmeyer, J. R. Heath, *Annu. Rev. Phys. Chem.* **1998**, *49*, 371.

[23]   S. M. Ilett, A. Orrock, W. C. K. Poon, P. N. Pusey, *Phys. Rev. E* **1995**, *51*, 1344.

[24]   M. Dijkstra, J. M. Brader, R. Evans, *J. Phys. Condens. Matter* **1999**, *11*, 10079.

[25]   R. van Roij, J.-P. Hansen, *Phys. Rev. Lett.* **1997**, *79*, 3082.

[26]   Y. Wang, Y. Wang, D. R. Breed, V. N. Manoharan, L. Feng, A. D. Hollingsworth, M. Weck, D. J. Pine, *Nature* **2012**, *491*, 51.

[27]   G. Chen, K. J. Gibson, D. Liu, H. C. Rees, J.-H. Lee, W. Xia, R. Lin, H. L. Xin, O. Gang, Y. Weizmann, *Nat. Mater.* **2018**, 1.

[28]   J. P. Rolland, B. W. Maynor, L. E. Euliss, A. E. Exner, G. M. Denison, J. M. DeSimone, *J. Am. Chem. Soc.* **2005**, *127*, 10096.

[29]   S. E. A. Gratton, P. D. Pohlhaus, J. Lee, J. Guo, M. J. Cho, J. M. DeSimone, *J. Controlled Release* **2007**, *121*, 10.

[30]   S. Sacanna, W. T. M. Irvine, P. M. Chaikin, D. J. Pine, *Nature* **2010**, *464*, 575.

[31]   W. Lee, A. Chan, M. A. Bevan, J. A. Lewis, P. V. Braun, *Langmuir* **2004**, *20*, 5262.

[32]   J. Zhuang, H. Wu, Y. Yang, Y. C. Cao, *J. Am. Chem. Soc.* **2007**, *129*, 14166.

[33]   C. B. Murray, S. Sun, W. Gaschler, H. Doyle, T. A. Betley, C. R. Kagan, *IBM J. Res. Dev.* **2001**, *45*, 47.

[34]   E. V. Shevchenko, D. V. Talapin, C. B. Murray, S. O'Brien, *J. Am. Chem. Soc.* **2006**, *128*, 3620.

[35]   A. Dong, X. Ye, J. Chen, C. B. Murray, *Nano Lett.* **2011**, *11*, 1804.

[36]   D. V. Talapin, E. V. Shevchenko, M. I. Bodnarchuk, X. Ye, J. Chen, C. B. Murray, *Nature* **2009**, *461*, 964.

[37] F. X. Redl, K.-S. Cho, C. B. Murray, S. O'Brien, *Nature* **2003**, *423*, 968.

[38] X. Ye, J. Chen, C. B. Murray, *J. Am. Chem. Soc.* **2011**, *133*, 2613.

[39] P. Bartlett, A. I. Campbell, *Phys. Rev. Lett.* **2005**, *95*, 128302.

[40] A. P. Alivisatos, K. P. Johnsson, X. Peng, T. E. Wilson, C. J. Loweth, M. P. Bruchez Jr., P. G. Schultz, *Nature* **1996**, *382*, 609.

[41] A separate DNA-NP construct was concurrently developed by Alivisatos et al. [Ref. 40] with a limited number of DNA strands per particle. This type of building block typically yields discrete clusters of particles that are more readily analogized to individual "molecules". While several interesting studies have arisen from this initial design, this work will not focus on these types of building blocks for the sake of brevity.

[42] S. Y. Park, D. Stroud, *Phys. Rev. B* **2003**, *67*, 212202.

[43] L. M. Demers, C. A. Mirkin, R. C. Mucic, R. A. Reynolds, R. L. Letsinger, R. Elghanian, G. Viswanadham, *Anal. Chem.* **2000**, *72*, 5535.

[44] E.-Y. Kim, J. Stanton, R. A. Vega, K. J. Kunstman, C. A. Mirkin, S. M. Wolinsky, *Nucleic Acids Res.* **2006**, *34*, e54.

[45] S. J. Hurst, A. K. R. Lytton-Jean, C. A. Mirkin, *Anal. Chem.* **2006**, *78*, 8313.

[46] J. J. Storhoff, R. Elghanian, C. A. Mirkin, R. L. Letsinger, *Langmuir* **2002**, *18*, 6666.

[47] H. D. Hill, J. E. Millstone, M. J. Banholzer, C. A. Mirkin, *ACS Nano* **2009**, *3*, 418.

[48] J. J. Storhoff, R. Elghanian, R. C. Mucic, C. A. Mirkin, R. L. Letsinger, *J. Am. Chem. Soc.* **1998**, *120*, 1959.

[49] R. A. Reynolds, C. A. Mirkin, R. L. Letsinger, *J. Am. Chem. Soc.* **2000**, *122*, 3795.

[50] T. A. Taton, G. Lu, C. A. Mirkin, *J. Am. Chem. Soc.* **2001**, *123*, 5164.

[51] Y. C. Cao, R. Jin, C. A. Mirkin, *Science* **2002**, *297*, 1536.

[52] H. D. Hill, C. A. Mirkin, *Nat Protoc.* **2006**, *1*, 324.

[53] D. G. Georganopoulou, L. Chang, J.-M. Nam, C. S. Thaxton, E. J. Mufson, W. L. Klein, C. A. Mirkin, *Proc. Natl. Acad. Sci.* **2005**, *102*, 2273.

[54] E. D. Goluch, J.-M. Nam, D. G. Georganopoulou, T. N. Chiesl, K. A. Shaikh, K. S. Ryu, A. E. Barron, C. A. Mirkin, C. Liu, *Lab. Chip* **2006**, *6*, 1293.

[55] R. Jin, G. Wu, Z. Li, C. A. Mirkin, G. C. Schatz, *J. Am. Chem. Soc.* **2003**, *125*, 1643.

[56] S.-J. Park, T. A. Taton, C. A. Mirkin, *Science* **2002**, *295*, 1503.

[57] J.-M. Nam, C. S. Thaxton, C. A. Mirkin, *Science* **2003**, *301*, 1884.

[58] D. A. Giljohann, D. S. Seferos, P. C. Patel, J. E. Millstone, N. L. Rosi, C. A. Mirkin, *Nano Lett.* **2007**, *7*, 3818.

[59] N. L. Rosi, D. A. Giljohann, C. S. Thaxton, A. K. R. Lytton-Jean, M. S. Han, C. A. Mirkin, *Science* **2006**, *312*, 1027.

[60] D. S. Seferos, D. A. Giljohann, H. D. Hill, A. E. Prigodich, C. A. Mirkin, *J. Am. Chem. Soc.* **2007**, *129*, 15477.

[61] J. I. Cutler, E. Auyeung, C. A. Mirkin, *J. Am. Chem. Soc.* **2012**, *134*, 1376.

[62] J. J. Storhoff, A. A. Lazarides, R. C. Mucic, C. A. Mirkin, R. L. Letsinger, G. C. Schatz, *J. Am. Chem. Soc.* **2000**, *122*, 4640.

[63] T. A. Taton, R. C. Mucic, C. A. Mirkin, R. L. Letsinger, *J. Am. Chem. Soc.* **2000**, *122*, 6305.

[64] J.-S. Lee, S. I. Stoeva, C. A. Mirkin, *J. Am. Chem. Soc.* **2006**, *128*, 8899.

[65] S. Y. Park, D. Stroud, *Phys. Rev. B* **2003**, *68*, 224201.

[66] S. Y. Park, J.-S. Lee, D. Georganopoulou, C. A. Mirkin, G. C. Schatz, *J. Phys. Chem. B* **2006**, *110*, 12673.

[67] S.-J. Park, A. A. Lazarides, J. J. Storhoff, L. Pesce, C. A. Mirkin, *J. Phys. Chem. B* **2004**, *108*, 12375.

[68] A. J. Kim, P. L. Biancaniello, J. C. Crocker, *Langmuir* **2006**, *22*, 1991.

[69] S. Y. Park, A. K. R. Lytton-Jean, B. Lee, S. Weigand, G. C. Schatz, C. A. Mirkin, *Nature* **2008**, *451*, 553.

[70] D. Nykypanchuk, M. M. Maye, D. van der Lelie, O. Gang, *Nature* **2008**, *451*, 549.

[71] R. J. Macfarlane, R. V. Thaner, K. A. Brown, J. Zhang, B. Lee, S. T. Nguyen, C. A. Mirkin, *Proc. Natl. Acad. Sci.* **2014**, *111*, 14995.

[72] H. Xiong, D. van der Lelie, O. Gang, *J. Am. Chem. Soc.* **2008**, *130*, 2442.

[73] H. Xiong, D. van der Lelie, O. Gang, *Phys. Rev. Lett.* **2009**, *102*, 015504.

[74] R. J. Macfarlane, B. Lee, M. R. Jones, N. Harris, G. C. Schatz, C. A. Mirkin, *Science* **2011**, *334*, 204.

[75] R. J. Macfarlane, M. N. O'Brien, S. H. Petrosko, C. A. Mirkin, *Angew. Chem. Int. Ed.* **2013**, *52*, 5688.

[76] The text and figures in Section 3 represent the highlights of achievable NP core identities (size, shape, and composition) and PAE crystallographic symmetries. While the list of examples is intended to be extensive, given the diverse breadth of research utilizing these building blocks, the cases mentioned may not be comprehensive.

[77] C. Zhang, R. J. Macfarlane, K. L. Young, C. H. J. Choi, L. Hao, E. Auyeung, G. Liu, X. Zhou, C. A. Mirkin, *Nat. Mater.* **2013**, *12*, 741.

[78] Y. Zhang, F. Lu, K. G. Yager, D. van der Lelie, O. Gang, *Nat. Nanotechnol.* **2013**, *8*, 865.

[79] J.-S. Lee, A. K. R. Lytton-Jean, S. J. Hurst, C. A. Mirkin, *Nano Lett.* **2007**, *7*, 2112.

[80] Y. Cao, R. Jin, C. A. Mirkin, *J. Am. Chem. Soc.* **2001**, *123*, 7961.

[81] G. P. Mitchell, C. A. Mirkin, R. L. Letsinger, *J. Am. Chem. Soc.* **1999**, *121*, 8122.

[82] D. Sun, O. Gang, *J. Am. Chem. Soc.* **2011**, *133*, 5252.

[83] D. Sun, O. Gang, *Langmuir* **2013**, *29*, 7038.

[84] J. I. Cutler, D. Zheng, X. Xu, D. A. Giljohann, C. A. Mirkin, *Nano Lett.* **2010**, *10*, 1477.

[85] K. L. Young, A. W. Scott, L. Hao, S. E. Mirkin, G. Liu, C. A. Mirkin, *Nano Lett.* **2012**, *12*, 3867.

[86] Y. Wang, Y. Wang, X. Zheng, É. Ducrot, M.-G. Lee, G.-R. Yi, M. Weck, D. J. Pine, *J. Am. Chem. Soc.* **2015**, *137*, 10760.

[87] P. H. Rogers, E. Michel, C. A. Bauer, S. Vanderet, D. Hansen, B. K. Roberts, A. Calvez, J. B. Crews, K. O. Lau, A. Wood, D. J. Pine, P. V. Schwartz, *Langmuir* **2005**, *21*, 5562.

[88] S. Lee, J. H. Yoon, I.-S. Jo, J. S. Oh, D. J. Pine, T. S. Shim, G.-R. Yi, *Langmuir* **2018**, *34*, 11042.

[89] É. Ducrot, M. He, G.-R. Yi, D. J. Pine, *Nat. Mater.* **2017**, *16*, 652.

[90] W. Morris, W. E. Briley, E. Auyeung, M. D. Cabezas, C. A. Mirkin, *J. Am. Chem. Soc.* **2014**, *136*, 7261.

[91] E. Auyeung, J. I. Cutler, R. J. Macfarlane, M. R. Jones, J. Wu, G. Liu, K. Zhang, K. D. Osberg, C. A. Mirkin, *Nat. Nanotechnol.* **2012**, *7*, 24.

[92] Y. Wang, I. C. Jenkins, J. T. McGinley, T. Sinno, J. C. Crocker, *Nat. Commun.* **2017**, *8*, 14173.

[93] Y. Wang, Y. Wang, X. Zheng, É. Ducrot, J. S. Yodh, M. Weck, D. J. Pine, *Nat. Commun.* **2015**, *6*, 7253.

[94] R. Dreyfus, M. E. Leunissen, R. Sha, A. V. Tkachenko, N. C. Seeman, D. J. Pine, P. M. Chaikin, *Phys. Rev. Lett.* **2009**, *102*, 048301.

[95] R. Dreyfus, M. E. Leunissen, R. Sha, A. Tkachenko, N. C. Seeman, D. J. Pine, P. M. Chaikin, *Phys. Rev. E* **2010**, *81*, 041404.

[96] R. J. Macfarlane, M. R. Jones, A. J. Senesi, K. L. Young, B. Lee, J. Wu, C. A. Mirkin, *Angew. Chem. Int. Ed.* **2010**, *49*, 4589.

[97] X. Xu, N. L. Rosi, Y. Wang, F. Huo, C. A. Mirkin, *J. Am. Chem. Soc.* **2006**, *128*, 9286.

WILEY-VCH

[98] S.-J. Park, A. A. Lazarides, C. A. Mirkin, R. L. Letsinger, *Angew. Chem. Int. Ed.* **2001**, *40*, 2909.

[99] J. R. McMillan, J. D. Brodin, J. A. Millan, B. Lee, M. Olvera de la Cruz, C. A. Mirkin, *J. Am. Chem. Soc.* **2017**, *139*, 1754.

[100] O. G. Hayes, J. R. McMillan, B. Lee, C. A. Mirkin, *J. Am. Chem. Soc.* **2018**, *140*, 9269.

[101] J. R. McMillan, C. A. Mirkin, *J. Am. Chem. Soc.* **2018**, *140*, 6776.

[102] W. Liu, M. Tagawa, H. L. Xin, T. Wang, H. Emamy, H. Li, K. G. Yager, F. W. Starr, A. V. Tkachenko, O. Gang, *Science* **2016**, *351*, 582.

[103] Y. Tian, Y. Zhang, T. Wang, H. L. Xin, H. Li, O. Gang, *Nat. Mater.* **2016**, *15*, 654.

[104] W. Liu, J. Halverson, Y. Tian, A. V. Tkachenko, O. Gang, *Nat. Chem.* **2016**, *8*, 867.

[105] M. R. Jones, R. J. Macfarlane, A. E. Prigodich, P. C. Patel, C. A. Mirkin, *J. Am. Chem. Soc.* **2011**, *133*, 18865.

[106] M. N. O'Brien, M. R. Jones, K. A. Brown, C. A. Mirkin, *J. Am. Chem. Soc.* **2014**, *136*, 7603.

[107] E. B. Mock, H. De Bruyn, B. S. Hawkett, R. G. Gilbert, C. F. Zukoski, *Langmuir* **2006**, *22*, 4037.

[108] J. S. DuChene, W. Niu, J. M. Abendroth, Q. Sun, W. Zhao, F. Huo, W. D. Wei, *Chem. Mater.* **2013**, *25*, 1392.

[109] B. D. Clark, C. R. Jacobson, M. Lou, J. Yang, L. Zhou, S. Gottheim, C. J. DeSantis, P. Nordlander, N. J. Halas, *Nano Lett.* **2018**, *18*, 1234.

[110] D. Lisjak, A. Mertelj, *Prog. Mater. Sci.* **2018**, *95*, 286.

[111] M. N. O'Brien, M. R. Jones, B. Lee, C. A. Mirkin, *Nat. Mater.* **2015**, *14*, 833.

[112] M. R. Jones, R. J. Macfarlane, B. Lee, J. Zhang, K. L. Young, A. J. Senesi, C. A. Mirkin, *Nat. Mater.* **2010**, *9*, 913.

[113] S. Vial, D. Nykypanchuk, K. G. Yager, A. V. Tkachenko, O. Gang, *ACS Nano* **2013**, *7*, 5437.

[114] F. Lu, K. G. Yager, Y. Zhang, H. Xin, O. Gang, *Nat. Commun.* **2015**, *6*, 6912.

[115] M. N. O'Brien, M. Girard, H.-X. Lin, J. A. Millan, M. O. de la Cruz, B. Lee, C. A. Mirkin, *Proc. Natl. Acad. Sci.* **2016**, *113*, 10485.

[116] V. N. Manoharan, M. T. Elsesser, D. J. Pine, *Science* **2003**, *301*, 483.

[116] While a plethora of core compositions, shapes, and sizes have been demonstrated, not all compositions are currently accessible in all size regimes or in all possible NP shapes.

[118] H. D. Hill, R. J. Macfarlane, A. J. Senesi, B. Lee, S. Y. Park, C. A. Mirkin, *Nano Lett.* **2008**, *8*, 2341.

[119] S. E. Seo, M. X. Wang, C. M. Shade, J. L. Rouge, K. A. Brown, C. A. Mirkin, *ACS Nano* **2016**, *10*, 1771.

[120] S. Pal, Y. Zhang, S. K. Kumar, O. Gang, *J. Am. Chem. Soc.* **2015**, *137*, 4030.

[121] T. Oh, S. S. Park, C. A. Mirkin, *Adv. Mater.* **n.d.**, *0*, 1805480.

[122] A. J. Senesi, D. J. Eichelsdoerfer, K. A. Brown, B. Lee, E. Auyeung, C. H. J. Choi, R. J. Macfarlane, K. L. Young, C. A. Mirkin, *Adv. Mater.* **2014**, *26*, 7235.

[123] R. V. Thaner, Y. Kim, T. I. N. G. Li, R. J. Macfarlane, S. T. Nguyen, M. Olvera de la Cruz, C. A. Mirkin, *Nano Lett.* **2015**, *15*, 5545.

[124] G. L. Miessler, P. J. Fischer, D. A. Tarr, *Inorganic Chemistry*, Pearson, Boston, **2013**.

[125] J. E. Jones, *Proc R Soc Lond A* **1924**, *106*, 463.

[126] M. Mohebifar, E. R. Johnson, C. N. Rowley, *J. Chem. Theory Comput.* **2017**, *13*, 6146.

[127] S. E. Seo, T. Li, A. J. Senesi, C. A. Mirkin, B. Lee, *J. Am. Chem. Soc.* **2017**, *139*, 16528.

[128] H. Xiong, M. Y. Sfeir, O. Gang, *Nano Lett.* **2010**, *10*, 4456.

[129] J. A. Mason, C. R. Laramy, C.-T. Lai, M. N. O'Brien, Q.-Y. Lin, V. P. Dravid, G. C. Schatz, C. A. Mirkin, *J. Am. Chem. Soc.* **2016**, *138*, 8722.

[130] S. Srivastava, D. Nykypanchuk, M. M. Maye, A. V. Tkachenko, O. Gang, *Soft Matter* **2013**, *9*, 10452.

[131] J. Zhu, Y. Kim, H. Lin, S. Wang, C. A. Mirkin, *J. Am. Chem. Soc.* **2018**, *140*, 5061.

[132] G. Bonner, A. M. Klibanov, *Biotechnol. Bioeng.* **2000**, *68*, 339.

[133] A. Arcella, G. Portella, R. Collepardo-Guevara, D. Chakraborty, D. J. Wales, M. Orozco, *J. Phys. Chem. B* **2014**, *118*, 8540.

[134] J. Srinivasan, T. E. Cheatham, P. Cieplak, P. A. Kollman, D. A. Case, *J. Am. Chem. Soc.* **1998**, *120*, 9401.

[135] M. M. Maye, M. T. Kumara, D. Nykypanchuk, W. B. Sherman, O. Gang, *Nat. Nanotechnol.* **2010**, *5*, 116.

[136] Y. Kim, R. J. Macfarlane, C. A. Mirkin, *J. Am. Chem. Soc.* **2013**, *135*, 10342.

[137] Y. Kim, R. J. Macfarlane, M. R. Jones, C. A. Mirkin, *Science* **2016**, *351*, 579.

[138] The crystallographic symmetry of a PAE lattice is defined by only the identity and relative placement of the NP cores, as opposed to the full hydrodynamic radius of the PAE.

[139] B. Srinivasan, T. Vo, Y. Zhang, O. Gang, S. Kumar, V. Venkatasubramanian, *Proc. Natl. Acad. Sci.* **2013**, *110*, 18431.

[140] A. V. Tkachenko, *Phys. Rev. Lett.* **2002**, *89*, 148303.

[141] T. Vo, V. Venkatasubramanian, S. Kumar, B. Srinivasan, S. Pal, Y. Zhang, O. Gang, *Proc. Natl. Acad. Sci.* **2015**, *112*, 4982.

[142] R. J. Macfarlane, M. R. Jones, B. Lee, E. Auyeung, C. A. Mirkin, *Science* **2013**, *341*, 1222.

[143] R. V. Thaner, I. Eryazici, R. J. Macfarlane, K. A. Brown, B. Lee, S. T. Nguyen, C. A. Mirkin, *J. Am. Chem. Soc.* **2016**, *138*, 6119.

[144] M. N. O'Brien, K. A. Brown, C. A. Mirkin, *ACS Nano* **2016**, *10*, 1363.

[145] Z. Jian, F. Chang, W. Ma, W. Yan, G. Yang, Y. Zhou, *Sci. China Ser. E Technol. Sci.* **2000**, *43*, 113.

[146] E. B. Moore, V. Molinero, *Nature* **2011**, *479*, 506.

[147] R. J. Macfarlane, B. Lee, H. D. Hill, A. J. Senesi, S. Seifert, C. A. Mirkin, *Proc. Natl. Acad. Sci.* **2009**, *106*, 10493.

[148] S. Dhakal, K. L. Kohlstedt, G. C. Schatz, C. A. Mirkin, M. Olvera de la Cruz, *ACS Nano* **2013**, *7*, 10948.

[149] E. Auyeung, T. I. N. G. Li, A. J. Senesi, A. L. Schmucker, B. C. Pals, M. O. de la Cruz, C. A. Mirkin, *Nature* **2014**, *505*, 73.

[150] G. Wulff, *Z. Für Krist. - Cryst. Mater.* **1901**, *34*, 449.

[151] S. E. Seo, M. Girard, M. O. de la Cruz, C. A. Mirkin, *Nat. Commun.* **2018**, *9*, 4558.

[152] M. N. O'Brien, H.-X. Lin, M. Girard, M. Olvera de la Cruz, C. A. Mirkin, *J. Am. Chem. Soc.* **2016**, *138*, 14562.

[153] T. Oh, J. C. Ku, J.-H. Lee, M. C. Hersam, C. A. Mirkin, *Nano Lett.* **2018**, *18*, 6022.

[154] J. C. Ku, M. B. Ross, G. C. Schatz, C. A. Mirkin, *Adv. Mater.* **2015**, *27*, 3159.

[155] N. K. Mahenderkar, Q. Chen, Y.-C. Liu, A. R. Duchild, S. Hofheins, E. Chason, J. A. Switzer, *Science* **2017**, *355*, 1203.

[156] M. N. O'Brien, B. Radha, K. A. Brown, M. R. Jones, C. A. Mirkin, *Angew. Chem.* **2014**, *126*, 9686.

[157] W. Zhou, Q.-Y. Lin, J. A. Mason, V. P. Dravid, C. A. Mirkin, *Small* **2018**, *14*, 1802742.

[158] Q.-Y. Lin, J. A. Mason, Z. Li, W. Zhou, M. N. O'Brien, K. A. Brown, M. R. Jones, S. Butun, B. Lee, V. P. Dravid, K. Aydin, C. A. Mirkin, *Science* **2018**, *359*, 669.

[159] D. J. Lewis, P. A. Gabrys, R. J. Macfarlane, *Langmuir* **2018**, *34*, 14842.

[160] B. D. Myers, Q.-Y. Lin, H. Wu, E. Luijten, C. A. Mirkin, V. P. Dravid, *ACS Nano* **2016**, *10*, 5679.

[161] A. J. Senesi, D. J. Eichelsdoerfer, R. J. Macfarlane, M. R. Jones, E. Auyeung, B. Lee, C. A. Mirkin, *Angew. Chem. Int. Ed.* **2013**, *52*, 6624.

[162] H. J. Frost, *Mater. Charact.* **1994**, *32*, 257.

[163] C. V. Thompson, H. J. Frost, F. Spaepen, *Acta Metall.* **1987**, *35*, 887.

[164] M. Ohring, *Materials Science of Thin Films: Deposition and Structure*, Academic Press, San Diego, CA, **2002**.

[165] S. L. Hellstrom, Y. Kim, J. S. Fakonas, A. J. Senesi, R. J. Macfarlane, C. A. Mirkin, H. A. Atwater, *Nano Lett.* **2013**, *13*, 6084.

[166] M. X. Wang, S. E. Seo, P. A. Gabrys, D. Fleischman, B. Lee, Y. Kim, H. A. Atwater, R. J. Macfarlane, C. A. Mirkin, *ACS Nano* **2017**, *11*, 180.

[167] P. A. Gabrys, S. E. Seo, M. X. Wang, E. Oh, R. J. Macfarlane, C. A. Mirkin, *Nano Lett.* **2018**, *18*, 579.

[168] R. Choudhury, D. R. Bowler, M. J. Gillan, *J. Phys. Condens. Matter* **2008**, *20*, 235227.

[169] W. L. Bragg, J. F. Nye, *Proc. R. Soc. Lond. Ser. Math. Phys. Sci.* **1947**, *190*, 474.

[170] A. S. Argon, H. Y. Kuo, *Mater. Sci. Eng.* **1979**, *39*, 101.

[171] J. W. Matthews, *J. Vac. Sci. Technol.* **1975**, *12*, 126.

[172] D. G. Stroppa, R. D. Righetto, L. A. Montoro, L. Houben, J. Barthel, M. A. Cordeiro, E. R. Leite, W. Weng, C. J. Kiely, A. J. Ramirez, *Nanoscale Res. Lett.* **2013**, *8*, 475.

[173] J. Kim, Z. Ou, M. R. Jones, X. Song, Q. Chen, *Nat. Commun.* **2017**, *8*, 761.

[174] J. Kim, M. R. Jones, Z. Ou, Q. Chen, *ACS Nano* **2016**, *10*, 9801.

[175] G. Antczak, G. Ehrlich, *Surf. Sci. Rep.* **2007**, *62*, 39.

[176] G. Antczak, G. Ehrlich, *Surface Diffusion: Metals, Metal Atoms, and Clusters*, Cambridge University Press, **2010**.

[177] K. Iwata, S. Yamazaki, P. Mutombo, P. Hapala, M. Ondráček, P. Jelínek, Y. Sugimoto, *Nat. Commun.* **2015**, *6*, 7766.

[178] N. de Jonge, F. M. Ross, *Nat. Nanotechnol.* **2011**, *6*, 695.

[179] B. R. Pauw, *J. Phys. Condens. Matter* **2013**, *25*, 383201.

[180] J. Kotakoski, C. Mangler, J. C. Meyer, *Nat. Commun.* **2014**, *5*, 3991.

[181] B. S. Swartzentruber, *Phys. Rev. Lett.* **1996**, *76*, 459.

[182] L. Zhong, F. Sansoz, Y. He, C. Wang, Z. Zhang, S. X. Mao, *Nat. Mater.* **2017**, *16*, 439.

[183] C. V. Thompson, *Annu. Rev. Mater. Sci.* **1990**, *20*, 245.

[184] K. Fujiwara, R. Maeda, K. Maeda, H. Morito, *Scr. Mater.* **2017**, *133*, 65.

[185] S. Tokita, H. Kokawa, Y. S. Sato, H. T. Fujii, *Mater. Charact.* **2017**, *131*, 31.

[186] D. J. Park, J. C. Ku, L. Sun, C. M. Lethiec, N. P. Stern, G. C. Schatz, C. A. Mirkin, *Proc. Natl. Acad. Sci.* **2017**, *114*, 457.

[187] D. J. Park, C. Zhang, J. C. Ku, Y. Zhou, G. C. Schatz, C. A. Mirkin, *Proc. Natl. Acad. Sci.* **2015**, *112*, 977.

[188] L. Sun, H. Lin, D. J. Park, M. R. Bourgeois, M. B. Ross, J. C. Ku, G. C. Schatz, C. A. Mirkin, *Nano Lett.* **2017**, *17*, 2313.

[189] H. Alaeian, J. A. Dionne, *Opt. Express* **2012**, *20*, 15781.

[190] M. B. Ross, M. G. Blaber, G. C. Schatz, *Nat. Commun.* **2014**, *5*, 4090.

[191] A. Myerson, *Handbook of Industrial Crystallization*, Butterworth-Heinemann, **2002**.

[192] W. L. Winterbottom, *Acta Metall.* **1967**, *15*, 303.

[193] W. Bao, W. Jiang, D. Srolovitz, Y. Wang, *SIAM J. Appl. Math.* **2017**, *77*, 2093.

[194] R. K. P. Zia, J. E. Avron, J. E. Taylor, *J. Stat. Phys.* **1988**, *50*, 727.

[195] B. Bhushan, D. Luo, S. R. Schricker, W. Sigmund, S. Zauscher, *Handbook of Nanomaterials Properties*, Springer Science & Business Media, **2014**.

[196] F. A. Cotton, G. Wilkinson, C. A. Murillo, M. Bochmann, *Advanced Inorganic Chemistry*, Wiley-Interscience, New York, **1999**.

[197] G. Bastard, *Wave Mechanics Applied to Semiconductor Heterostructures*, Les Éditions De Physique, **1988**.

[198] J. E. Ayers, T. Kujofsa, P. Rago, J. Raphael, *Heteroepitaxy of Semiconductors: Theory, Growth, and Characterization, Second Edition*, CRC Press, **2016**.

[199] D. V. Morgan, K. Board, *An Introduction to Semiconductor Microtechnology*, J. Wiley, Chichester; New York, **1990**.

[200] R. C. Mucic, J. J. Storhoff, C. A. Mirkin, R. L. Letsinger, *J. Am. Chem. Soc.* **1998**, *120*, 12674.

[201] J. B. Lassiter, H. Sobhani, J. A. Fan, J. Kundu, F. Capasso, P. Nordlander, N. J. Halas, *Nano Lett.* **2010**, *10*, 3184.

[202] S. Strauf, *Nat. Photonics* **2011**, *5*, 72.

[203] A. D. Lantada, A. de B. Romero, M. Schwentenwein, C. Jellinek, J. Homa, *Smart Mater. Struct.* **2016**, *25*, 054015.

[204] A. Fernández-Pacheco, R. Streubel, O. Fruchart, R. Hertel, P. Fischer, R. P. Cowburn, *Nat. Commun.* **2017**, *8*, 15756.

[205] J.-H. Choi, H. Wang, S. J. Oh, T. Paik, P. Sung, J. Sung, X. Ye, T. Zhao, B. T. Diroll, C. B. Murray, C. R. Kagan, *Science* **2016**, *352*, 205.

[206] K. L. Kelly, E. Coronado, L. L. Zhao, G. C. Schatz, *J. Phys. Chem. B* **2003**, *107*, 668.

[207] T. Lee, J. Jang, H. Jeong, J. Rho, *Nano Converg.* **2018**, *5*, 1.

[208] U. S. Inan, A. Inan, *Electromagnetic Waves*, Prentice Hall, Upper Saddle River, N.J, **1999**.

[209] S. R. Cherry, J. A. Sorenson, M. E. Phelps, *Physics in Nuclear Medicine*, Elsevier Health Sciences, **2012**.

[210] R. C. Schroden, M. Al-Daous, C. F. Blanford, A. Stein, *Chem. Mater.* **2002**, *14*, 3305.

[211] S. Peng, R. Zhang, V. H. Chen, E. T. Khabiboulline, P. Braun, H. A. Atwater, *ACS Photonics* **2016**, *3*, 1131.

[212] M. K. Bhuyan, A. Soleilhac, M. Somayaji, T. E. Itina, R. Antoine, R. Stoian, *Sci. Rep.* **2018**, *8*, 9665.

[213] A. Dinwiddie, R. Null, M. Pizzano, L. Chuong, A. Leigh Krup, H. Ee Tan, N. H. Patel, *Dev. Biol.* **2014**, *392*, 404.

[214] Z.-Z. Gu, H. Uetsuka, K. Takahashi, R. Nakajima, H. Onishi, A. Fujishima, O. Sato, *Angew. Chem. Int. Ed.* **2003**, *42*, 894.

[215] Y. Zhao, Z. Xie, H. Gu, C. Zhu, Z. Gu, *Chem. Soc. Rev.* **2012**, *41*, 3297.

[216] L. Sun, H. Lin, K. L. Kohlstedt, G. C. Schatz, C. A. Mirkin, *Proc. Natl. Acad. Sci.* **2018**, *115*, 7242.

[217] N. W. Ashcroft, N. D. Mermin, *Solid State Physics*, Cengage Learning, New York, **1976**.

[218] C. Diaz-Egea, T. Ben, M. Herrera, J. Hernández, E. Pedrueza, J. L. Valdés, J. P. Martínez-Pastor, F. Attouchi, Z. Mafhoud, O. Stéphan, S. I. Molina, *Nanotechnology* **2015**, *26*, 405702.

[219] W. Cai, V. Shalaev, *Optical Metamaterials: Fundamentals and Applications*, Springer Science & Business Media, **2009**.

[220] S. J. Barrow, X. Wei, J. S. Baldauf, A. M. Funston, P. Mulvaney, *Nat. Commun.* **2012**, *3*, 1275.

[221] S. J. Barrow, A. M. Funston, X. Wei, P. Mulvaney, *Nano Today* **2013**, *8*, 138.

[222] R. H. Tarkanyan, D. G. Niarchos, *Opt. Express* **2006**, *14*, 5433.

[223] T. Ito, S. Okazaki, *Nature* **2000**, *406*, 1027.

[224] V. R. Manfrinato, L. Zhang, D. Su, H. Duan, R. G. Hobbs, E. A. Stach, K. K. Berggren, *Nano Lett.* **2013**, *13*, 1555.

[225] P. Hajiyev, C. Cong, C. Qiu, T. Yu, *Sci. Rep.* **2013**, *3*, 2593.

[226] D. Zhao, D. Schneider, G. Fytas, S. K. Kumar, *ACS Nano* **2014**, *8*, 8163.

[227] W. Kim, J. Zide, A. Gossard, D. Klenov, S. Stemmer, A. Shakouri, A. Majumdar, *Phys. Rev. Lett.* **2006**, *96*, 045901.

[228] X. C. Tong, *Functional Metamaterials and Metadevices*, Springer, **2017**.

[229] L. Jiang, B. Gu, H. Hu, *Compos. Struct.* **2016**, *135*, 23.

[230] Z. Wang, A. Zulifqar, H. Hu, in *Adv. Compos. Mater. Aerosp. Eng.* (Eds: S. Rana, R. Fangueiro), Woodhead Publishing, **2016**, pp. 213–240.

[231] Z. Zhang, S. C. Glotzer, *Nano Lett.* **2004**, *4*, 1407.

[232] E. Maciá, *Rep. Prog. Phys.* **2006**, *69*, 397.

[233] D. Mousanezhad, B. Haghpanah, R. Ghosh, A. M. Hamouda, H. Nayeb-Hashemi, A. Vaziri, *Theor. Appl. Mech. Lett.* **2016**, *6*, 81.

[234] M. C. Gao, J.-W. Yeh, P. K. Liaw, Y. Zhang, *High-Entropy Alloys: Fundamentals and Applications*, Springer, **2016**.

[235] E. Auyeung, R. J. Macfarlane, C. H. J. Choi, J. I. Cutler, C. A. Mirkin, *Adv. Mater.* **2012**, *24*, 5181.

[236] W. Cheng, M. J. Campolongo, J. J. Cha, S. J. Tan, C. C. Umbach, D. A. Muller, D. Luo, *Nat. Mater.* **2009**, *8*, 519.
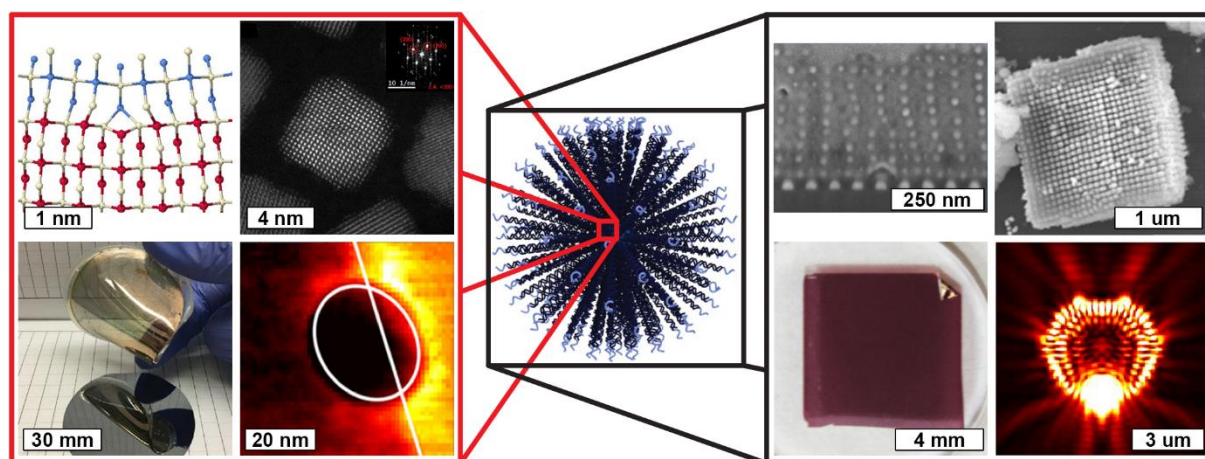
Figure 1. DNA-grafted nanoparticles as "programmable atom equivalents" utilize atomic crystallization phenomena as a framework to build nanoparticle superlattices at larger length scales. Adapted with permission.[152,154,155,167,168,172,186,218] Copyright 2016, 2018, American Chemical Society (ACS). Copyright 2015, John Wiley and Sons. Copyright 2017, The American Association for the Advancement of Science (AAAS). Copyright 2008 and 2015, IOP Publishing. Copyright 2013, Springer Nature. Copyright 2017, National Academy of Sciences (NAS).
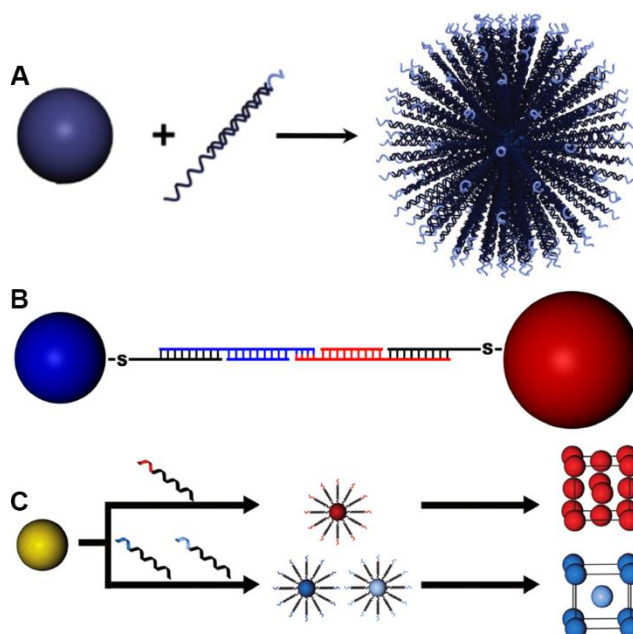
Figure 2. The characteristics of a DNA-grafted nanoparticle that allow it to be defined as a "programmable atom equivalent" are as follows: (A) a densely functionalized core that results in multivalency, (B) a "sticky end" motif that provides specific binding interactions between complementary particles, and (C) a programmable crystalline unit cell that is based on maximizing complementary contact. Adapted with permission.[74,75] Copyright 2011, AAAS. Copyright 2013, John Wiley and Sons.
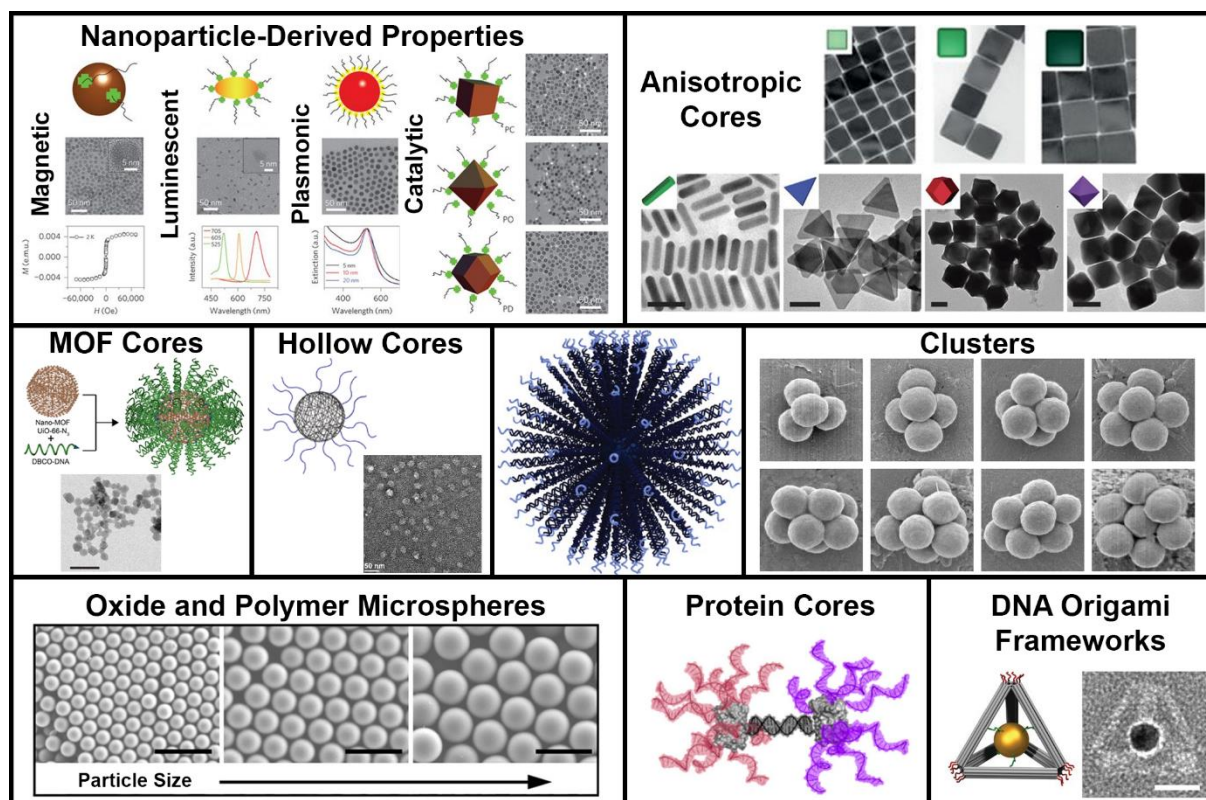
Figure 3. A modular nanoparticle core provides "programmable atom equivalents" with a breadth of compositions, sizes, and shapes (directional binding) yielding a wide array of different properties and characteristics. Adapted with permission.[78,86,90,91,100,102,111,112,116]

Figure 4. Both (A) atoms and (B) "programmable atom equivalents" analogously exhibit well-defined energy potentials based on interparticle distance, resulting in equilibrium bond lengths. Adapted with permission.[126,127] Copyright 2017, ACS.
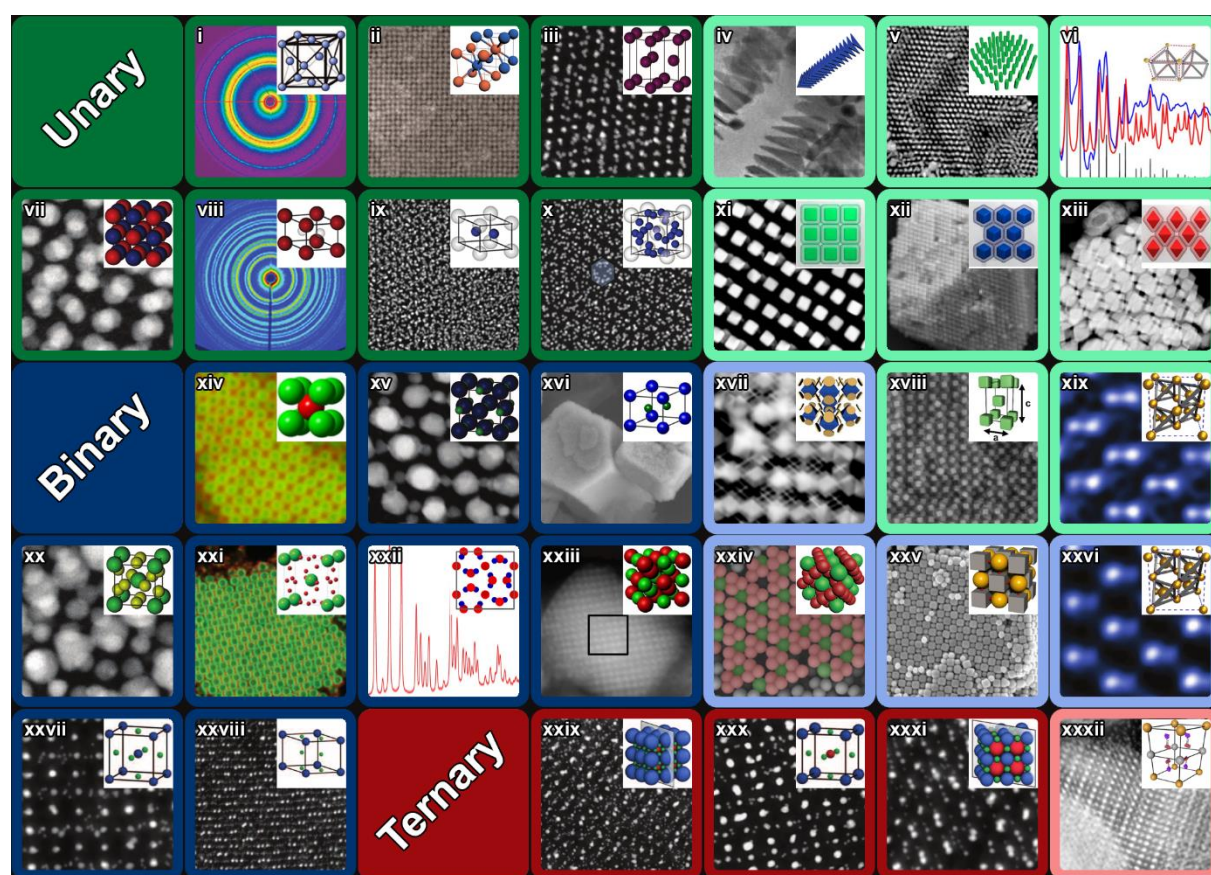
Figure 5. Specific and programmable binding, dictated by the DNA coronae, enables numerous crystallographic unit cell symmetries for "programmable atom equivalents," including (i) face-centered cubic (fcc), (ii) body-centered cubic (bcc), (iii) hexagonal close-packed (hcp), (iv) 1D chains, (v) 2D lamella, (vi) simple hexagonal, (vii) simple cubic (sc), (viii) simple hexagonal, (ix) graphite-type, (x) lattice X, (xi) sc, (xii) fcc, (xiii) bcc, (xiv) CsCl, (xv) NaCl, (xvi) AlB_2, (xvii) complex fcc cocrystals involving multiple particle shapes, (xviii) body-centered tetragonal (bct), (xix) diamond, (xx) Cr_3Si, (xxi) Cs_6C_{60}, (xxii) Th_3P_4, (xxiii) NaTl, (xxiv) $MgCu_2$, (xxv) NaCl, (xxvi) zinc blende, (xxvii) A_2B_3, (xxviii) AB_4, (xxix) ABC_{12}, (xxx) ABC_3 face-type perovskite, (xxxi) ABC_3 edge-type perovskite, and (xxxii) layered simple hexagonal. Unary lattices (one nanoparticle core type) are denoted in green, binary (two core types) in blue, and ternary (three core types) in red. Dark colors (left) signify lattices created using isotropic

nanoparticle cores, light colors (right) signify lattices synthesized from nanoparticles with derived directional binding. Adapted with permission.[69,70,74,86,89,91–93,100,102,103,111,112,114,115,118,142,143,151,152,166] Copyright 2008, 2010, 2011, 2015, 2016, 2017, and 2018, Springer Nature. Copyright 2011, 2013, and 2016, AAAS. Copyright 2008, 2015, 2016, 2017, and 2018, ACS. Copyright 2016, NAS.
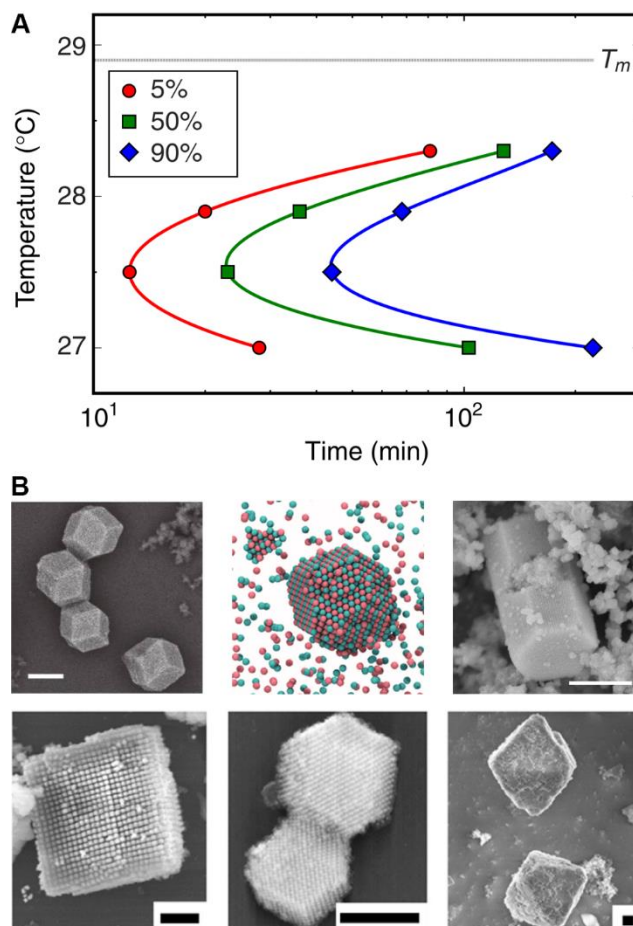

Figure 6. Atomic nucleation and growth behavior is mimicked by "programmable atom equivalents," resulting in (A) Time-Temperature-Transformation curves, and (B) well-defined crystallite habits based on the Wulff construction. All scale bars are 1 μm. Adapted with permission.[93,149,151–153] Copyright 2013, 2015, and 2018, Springer Nature. Copyright 2016 and 2018, ACS.
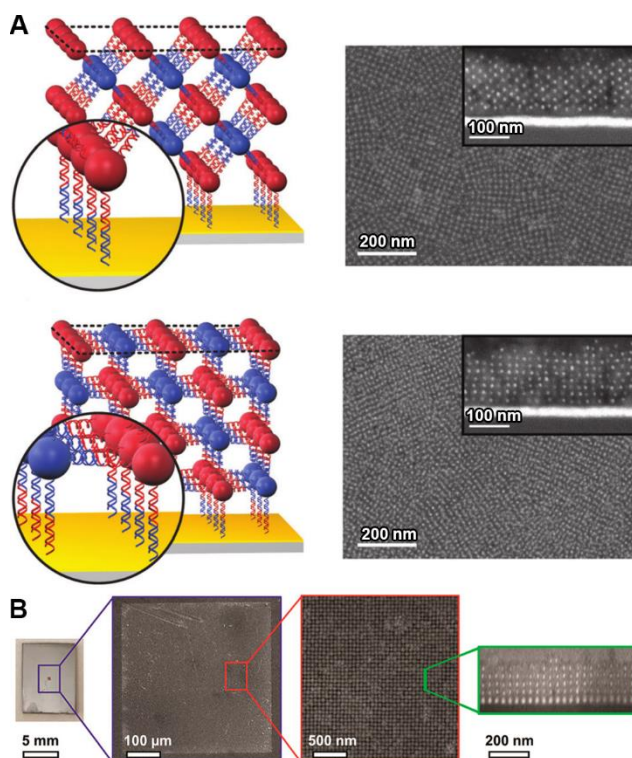
Figure 7. "Programmable atom equivalents" mimic atomic behavior at interfaces enabling (A) thin film crystallization and preferential grain alignment and (B) epitaxial growth. Adapted with permission.[161,166] Copyright 2013, John Wiley and Sons. Copyright 2017, ACS.
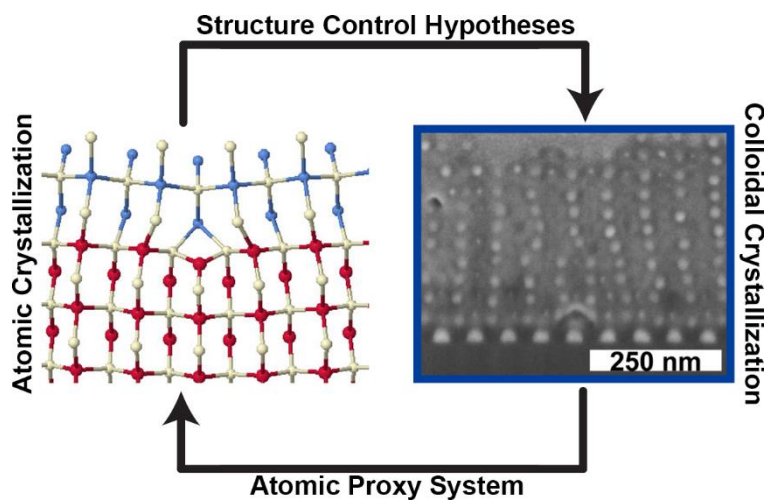
Figure 8. The strong structural analogies between atomic and "programmable atom equivalent" crystal formation allows for both atomic systems to provide hypothesis inspiration for colloidal crystallization and for "programmable atom equivalents" to be used as a proxy system for atomic crystallization. Adapted with permission.[167,168] Copyright 2008, IOP Publishing. Copyright 2018, ACS.
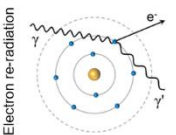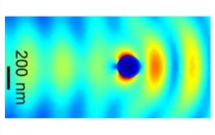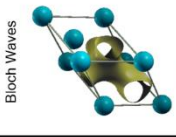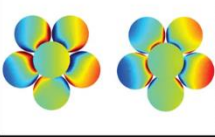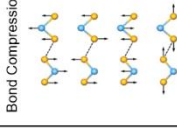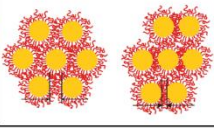
Figure 9. (Top) Optical, (middle) electrical, and (bottom) mechanical properties of materials can be manipulated at both the (left) atomic scale and (right) nanoscale, yielding different physical phenomena depending on the length scale of the ordering. Adapted with permission.[209,212,220,225,236] Copyright 2009, 2012, 2013, and 2018, Springer Nature. Copyright 2012, Elsevier. Courtesy of L Paulatto.

Biographies

Paul A. Gabrys received his B.S. in chemical engineering from the University of Rochester (UR) in 2015. He is currently an NSF graduate research fellow in the laboratory of Prof. Robert J. Macfarlane at the Massachusetts Institute of Technology (MIT) pursuing his PhD in materials science and engineering. His current research focuses on exploring classic materials science behaviors of DNA-directed nanoparticle assembly, particularly at interfaces.

Leonardo Zaborowski Zornberg received his B.S in Chemical Engineering from the California Institute of Technology in 2016. He is currently an NSF graduate research fellow and PhD candidate in the Department of Materials Science and Engineering at MIT in the Macfarlane Lab. His current research is on the optical response of self-assembling nanoscale systems, for both optical processing techniques and optical nanomaterials.

Rob Macfarlane received his Ph.D. in chemistry from Northwestern University in 2013. Since 2015, he has been an assistant professor of materials science at the Massachusetts Institute of Technology. His current research interests focus on the development of methods to synthesize hierarchically ordered polymer, nanoparticle, and biomaterial composite architectures via supramolecular-chemistry directed self-assembly.

The unique characteristics of DNA-grafted colloids enable the design and synthesis of nanoparticle-based crystals by drawing on well-understood atomic crystallization phenomena to understand and explain particle assembly behavior. This review explores how these "programmable atom equivalents" are a unique tool to rationally design and synthesize complex nano and microstructured materials.

Self-Assembly

P. A. Gabrys, L. Z. Zornberg, R. J. Macfarlane*

Programmable Atom Equivalents: Atomic Crystallization as a Framework for Synthesizing Nanoparticle Superlattices